

Theory of Spin Hall Effects in Semiconductors

Hans-Andreas Engel, Emmanuel I. Rashba, and Bertrand I. Halperin

2nd December 2024

Department of Physics, Harvard University, Cambridge, Massachusetts 02138

Abstract

Spin Hall effects are a collection of phenomena, resulting from spin-orbit coupling, in which an electrical current flowing through a sample can lead to spin transport in a perpendicular direction and spin accumulation at lateral boundaries. These effects, which do not require an applied magnetic field, can originate in a variety of intrinsic and extrinsic spin-orbit coupling mechanisms and depend on geometry, dimension, impurity scattering, and carrier density of the system—making the analysis of these effects a diverse field of research. In this article, we give an overview of the theoretical background of the spin Hall effects and summarize some of the most important results. First, we explain effective spin-orbit Hamiltonians, how they arise from band structure, and how they can be understood from symmetry considerations; including intrinsic coupling due to bulk inversion or structure asymmetry or due to strain, and extrinsic coupling due to impurities. This leads to different mechanisms of spin transport: spin precession, skew scattering, and side jump. Then we present the kinetic (Boltzmann) equations, which describe the spin-dependent distribution function of charge carriers, and the diffusion equation for spin polarization density. Next, we define the notion of spin currents and discuss their relation to spin polarization. Finally, we explain the electrically induced spin effects; namely, spin polarization and currents in bulk and near boundaries (the focus of most current theoretical research efforts), and spin injection, as well as effects in mesoscopic systems and in edge states.

Keywords: spin transport, spin Hall effect, spin accumulation, spin current, intrinsic spin-orbit coupling, extrinsic spin-orbit coupling, skew scattering, side-jump mechanism, semiconductors, graphene

1 Introduction

In the simplest version of a spin Hall effect, an electrical current passes through a sample with spin-orbit interaction, and induces a spin polarization near the lateral edges, with opposite polarization at opposing edges (D'yakonov and Perel', 1971). This effect does not require an external magnetic field or magnetic order in the equilibrium state before the current is applied. If conductors are connected to the

lateral edges, spin currents can be injected into them. Electrical current in a sample can also produce a bulk spin polarization, far from the edges, which is not generally classified *per se* as a spin Hall effect, though it is intimately related and is an important ingredient of spin Hall calculations.

Spin Hall effects have received a great deal of theoretical attention recently, in part because the subject includes ingredients of spintronics, electrical generation, transport, and control of nonequilibrium spin populations, and also because analysis has shown that the problem has remarkable subtlety. Theoretical efforts were also fueled by recent experimental observations of these effects.

In the following we consider semiconductors, where the various mechanisms of spin-orbit coupling are well-known and can be roughly classified into two categories. First, the extrinsic mechanism is only present in the vicinity of impurities and leads to spin-dependent scattering, including Mott skew scattering. Second, the intrinsic spin-orbit coupling remains finite away from impurities and can be understood as a (often spatially homogeneous) spin-orbit field inherent in the band structure. Furthermore, the spin-orbit couplings are strongly symmetry dependent and are therefore different for electron and for hole carriers, and are different for two and three dimensional systems. Thus, the microscopic processes involved in generating a spin Hall effect can depend critically on such system properties. Initially, there was hope that spin transport theory can be formulated in terms of universal spin currents that would simplify our understanding; however, it turned out that there is no such universality. As there is no unique description of the spin Hall effect, we should rather refer to it as a set of spin Hall effects.

There is already a vast amount of theoretical literature available on spin Hall effects and on the related spin currents. It is beyond the scope of this article to provide a historical overview or to give an explanation of all the theoretical techniques used. We rather provide an overview of the various mechanisms, explain them using intuitive and qualitative physical pictures, and give a summary of some key theoretical descriptions and results.

In contrast, the number of experiments on spin Hall effects is small and an overview is straightforward. In the experiment by Kato *et al.* (2004b), electrical currents in three-dimensional *n*-GaAs layers ($2\mu\text{m}$ thick) induced a spin Hall effect, which was optically detected via Kerr microscopy. Measurements in strained samples showed little dependence of the effect on the crystal orientation and it was concluded that the extrinsic mechanism proposed by D'yakonov and Perel' (1971) was causing the spin Hall effect (Kato *et al.*, 2004b). Indeed, the experimental data can be described with reasonable accuracy by the extrinsic mechanism in a model based on scattering by screened Coulomb impurities (Engel *et al.*, 2005), as well as one based on short-range scatterers (Tse and Das Sarma, 2006). (See Sec. 4.3.) Similar experiments in ZnSe (Stern *et al.*, 2006) were also in agreement with theory, and a spin Hall effect was observed at room temperature. In another experiment, Wunderlich *et al.* (2005) observed a spin Hall effect in two-dimensional layers of *p*-GaAs by detecting the polarization of recombination radiation at the edges of the sample. They ascribed this effect to the intrinsic mechanism, which is consistent with the magnitude of the observation (Schliemann and Loss, 2005; Nomura *et al.*, 2005). Furthermore, in measurements on a two-dimensional electron system in an AlGaAs

quantum well, a spin Hall effect was also observed and ascribed to the extrinsic mechanism (Sih *et al.*, 2005). Finally, Valenzuela and Tinkham (2006) observed a reciprocal spin Hall effect in Al, where a spin current induced a transverse voltage via the extrinsic mechanism (Hirsch, 1999).

In addition to theoretical works in the traditional sense, there is also a large amount of numerical simulations on concrete realizations of disordered systems, e.g., on a finite lattice. It has generally been difficult to make direct comparisons between numerical simulations and theoretical predictions, in part because theoretical works usually assume that the spin-orbit splittings are much less than the Fermi energy, while simulations tend to employ larger spin orbit splittings in order to obtain numerically significant results. See for example (Ando and Tamura, 1992; Sheng, Sheng and Ting, 2005; Nikolić *et al.*, 2005; Li *et al.*, 2005).

In Section 2 below, we review the mechanisms for spin-orbit coupling in the semiconductors of interest, and we discuss forms of the effective Hamiltonians that describe the carriers in various situations. In Section 3, we see how the various effective Hamiltonians can influence spin transport and accumulation. We discuss spin precession, produced by the intrinsic spin-orbit coupling, as well as skew scattering and the so-called side-jump effect, resulting from the extrinsic spin-orbit coupling. We introduce Boltzmann-type kinetic equations which can describe spin-transport and accumulation in various situations, and we discuss the simpler spin and charge diffusion equations which can typically be used in situations where the spin relaxation rate is much slower than momentum relaxation.

In Section 4, we discuss explicitly the spin polarization and spin transport arising from an electrical current in a semiconductor with spin-orbit coupling. We introduce the notion of a spin current and the spin Hall conductivity, and we discuss results that have been obtained for these quantities in various situations. We also discuss a relation between the spin Hall conductivity and the so-called anomalous Hall effect that can result from spin-orbit coupling in a ferromagnet or in semiconductor with a spin polarization induced by an external magnetic field.

Spin currents are not directly observed in experiments, however. If spin relaxation rates are slow, one may expect that spin-currents with a non-zero divergence can lead to observable local spin polarizations, in which relaxation of excess spin balances the accumulation of spin that is transported into a region by the spin current. Furthermore, boundary effects may be important and non-trivial; in the presence of an electric current, spin-polarization may be generated directly at a sample boundary. These issues are discussed in Subsection 4.5. We also discuss briefly mesoscopic systems, where all parts of the sample are close to a boundary.

A different type of spin Hall effect, associated with edge states, has been predicted to occur in certain systems that are insulating in the bulk, where the topology of the band structure has been altered due to spin orbit coupling. In Section 5, we discuss this concept, along with the possibility that such effects may occur and be observable in graphene sheets.

2 Spin-orbit coupling in semiconductors

For a non-relativistic electron in vacuum, the Dirac equation can be reduced to the Pauli equation, describing a two-component spinor and containing the Zeeman term. The Pauli equation also contains relativistic corrections—including the spin-orbit coupling

$$H_{\text{SO, vac}} = \lambda_{\text{vac}} \boldsymbol{\sigma} \cdot (\mathbf{k} \times \nabla \tilde{V}). \quad (1)$$

Here, we used $\lambda_{\text{vac}} = -\hbar^2/4m_0^2c^2 \approx -3.7 \times 10^{-6} \text{ \AA}^2$, vacuum electron mass m_0 , velocity of light c , and $\mathbf{k} = \mathbf{p}/\hbar$. In a semiconductor, we split the total potential $\tilde{V} = V_{\text{cr}} + V$ into the periodic crystal potential V_{cr} and an aperiodic part V , which contains the potential due to impurities, confinement, boundaries, and external electrical field. One then tries to eliminate the crystal potential as much as possible and to describe the charge carriers in terms of the band structure. The simplest systems of this sort can be exemplified by electrons in cubic direct-gap semiconductors. Then, the minimum of the energy spectrum is usually near the center of the Brillouin zone, and the two-fold Kramers degeneracy is the only degeneracy of the spectrum at $k = 0$. It follows from symmetry arguments, that for slow electrons in such crystals, and for slow carriers (electrons and holes) in high symmetry two-dimensional systems, the effective single-particle Hamiltonian is

$$H_{\text{eff}} = \epsilon_k + V + H_{\text{int}} + H_{\text{ext}}, \quad (2)$$

$$H_{\text{int}} = -\frac{1}{2} \mathbf{b}(\mathbf{k}) \cdot \boldsymbol{\sigma}, \quad (3)$$

$$H_{\text{ext}} = \lambda \boldsymbol{\sigma} \cdot (\mathbf{k} \times \nabla V), \quad (4)$$

where \mathbf{k} is the crystal wave vector relative to the zone center, and we assumed that V is only slowly varying on the scale of the lattice constant. Here $\boldsymbol{\sigma}$ is the vector of Pauli matrices for the pseudo spin- $\frac{1}{2}$ of the Kramer's doublet at $k = 0$; it is customary called a spin- $\frac{1}{2}$ system. $\mathbf{b}(\mathbf{k})$ is the intrinsic spin-orbit field, with $\mathbf{b}(\mathbf{k}) = -\mathbf{b}(-\mathbf{k})$ due to time reversal symmetry. Thus, for a three-dimensional system, \mathbf{b} can only be present if the inversion symmetry of the host crystal is broken. In the case of a two-dimensional system, it is conventional to talk about its two-dimensional bandstructure, and to include the confinement potential in ϵ_k and $\mathbf{b}(\mathbf{k})$ (instead of including it explicitly in V); in this case \mathbf{b} can also result from an asymmetry in the confinement.

In contrast, H_{ext} does not require broken inversion symmetry of the pure crystal or of the structure. It is important to note that λ in Equation (4) can be many orders of magnitude larger than the vacuum value λ_{vac} ; this is due to the large spin-orbit interaction when the Bloch electrons move close to the nuclei, with velocities that are close to relativistic. Both H_{int} and H_{ext} may be important for the spin Hall effect, as we will discuss in this article. We present specific forms of these effective Hamiltonians in Secs. 2.3 and 2.4.

2.1 Band structure of materials with spin-orbit interaction

We now consider the electron wavefunctions near the forbidden gap of a semiconductor. These wave functions are often described by the Kohn-Luttinger $\mathbf{k} \cdot \mathbf{p}$ method, where one expands the Hamiltonian in terms of band edge Bloch functions. Here, we present a brief overview of this method; more detailed explanations can be found, e.g., in Blount's (1962) review article or in the books by Bir and Pikus (1974) and by Winkler (2003).

For a given \mathbf{k} , the solutions of the Schrödinger equation are Bloch functions $e^{i\mathbf{k}\cdot\mathbf{r}}u_{\nu',\mathbf{k}}(\mathbf{r})$. Here, ν' is the band index and includes the spin degree of freedom. The lattice-periodic part $u_{\nu',\mathbf{k}}(\mathbf{r})$ of these Bloch functions can be expanded in the functions $u_{\nu,\mathbf{k}=0}(\mathbf{r}) = \langle \mathbf{r} | u_{\nu,0} \rangle$, which provide a complete basis when all bands ν are taken. For semiconductors with a direct gap at the center of the Brillouin zone, which we discuss here, one may consider states in close vicinity of $\mathbf{k} = 0$, truncate this expansion, and only take the closest bands into account. Therefore, it is sufficient to know the matrix elements of the full Hamiltonian H in the truncated basis $|\phi_\nu\rangle = e^{i\mathbf{k}\cdot\mathbf{r}}|u_{\nu,0}\rangle$, i.e., one considers $H_{\nu\nu'}(\mathbf{k}) = \langle \phi_\nu | H | \phi_{\nu'} \rangle$. More concretely, one evaluates

$$H_{\nu\nu'}(\mathbf{k}) = E_\nu \delta_{\nu\nu'} + \frac{\hbar^2 k^2}{2m_0} \delta_{\nu\nu'} + \frac{\hbar}{m_0} \mathbf{k} \cdot \langle u_{\nu,0} | \boldsymbol{\pi} | u_{\nu',0} \rangle, \quad (5)$$

where E_ν is the energy offset of the band at $\mathbf{k} = 0$, i.e., $[p^2/2m_0 + V_{\text{cr}} + (\lambda_{\text{vac}}/\hbar) \boldsymbol{\sigma} \cdot (\mathbf{p} \times \nabla V_{\text{cr}})] |u_{\nu,0}\rangle = E_\nu |u_{\nu,0}\rangle$. Further, $\boldsymbol{\pi} = \mathbf{p} + (\lambda_{\text{vac}}/\hbar) (\nabla V_{\text{cr}} \times \boldsymbol{\sigma})$, and one usually approximates $\boldsymbol{\pi} \approx \mathbf{p}$; then the last term of Equation (5) is proportional to the matrix element of $\mathbf{k} \cdot \mathbf{p}$, giving this method its name. Finally, this finite-dimensional Hamiltonian $H(\mathbf{k})$ now describes the band structure in terms of a few parameters—band offsets and momentum matrix elements of $\mathbf{k} = 0$ Bloch functions—and is well suited for analyzing charge carriers.

Alternatively, one can use a second method and construct a Hamiltonian by allowing all contributions (up to some order in k) that are invariant under the symmetry operations of the system—the coupling constants are material-dependent parameters. For example, when considering the top of the valence band in Fig. 1 and in the absence of inversion asymmetry, magnetic field, and strain, the most general form up to quadratic terms in k (i.e., in the effective mass approximation), is the 4×4 Luttinger Hamiltonian,

$$H_{\text{L}} = \frac{\hbar^2}{m_0} \left[\left(\gamma_1 + \frac{5}{2} \gamma_2 \right) \frac{k^2}{2} - \gamma_3 (\mathbf{k} \cdot \mathbf{J})^2 + (\gamma_3 - \gamma_2) \sum_i k_i^2 J_i^2 \right], \quad (6)$$

which is consistent with the cubic symmetry. Here, $\mathbf{J} = (J_x, J_y, J_z)$ and J_i are the angular momentum matrices for spin $\frac{3}{2}$, and γ_i are the material-dependent Luttinger parameters. H_{L} describes p -doped Si and Ge; for GaAs, due to broken inversion symmetry, terms linear in k arise as well.

By contrast, using the first method ($\mathbf{k} \cdot \mathbf{p}$ method) instead, the Hamiltonian $H_{\nu\nu'}(\mathbf{k})$ [Equation (5)] is evaluated directly for the eight bands ν (including spin) shown in Fig. 1, and one arrives at the simplest version of the 8×8 Kane model. It

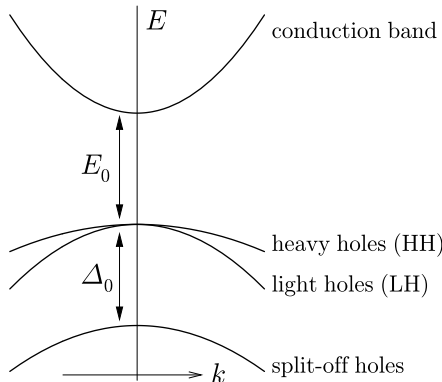


Figure 1: Schematic band structure of a cubic direct gap semiconductor. When spin-orbit interaction is disregarded, one finds an s -like conduction band and a p -like three-fold degenerate valence band. The spin-orbit interaction due to crystal potential V_{cr} [entering as \tilde{V} in Equation (1)] partially lifts this degeneracy and leads to a substantial splitting between the valence bands with total angular momentum $J = 3/2$ (heavy and light holes) and those with $J = 1/2$ (split-off holes).

only includes three parameters, namely, the energy gap E_0 , the energy of the split-off holes Δ_0 , and the matrix element P of the momentum (multiplied by \hbar/m_0) between s - and p -type states. P is nearly universal for III-V compounds, while the other parameters depend on the material. This eight-dimensional description is accurate for narrow band materials; for wider gaps it still provides understanding at a qualitative level.

Furthermore, one can then derive an effective, lower-dimensional Hamiltonian by block-diagonalizing $H_{\nu\nu'}$, this is an efficient way to calculate the band structure in the vicinity of $\mathbf{k} = 0$. One can do this either exactly or by using time-independent degenerate perturbation theory (see Sec. 2.2). Considering a particular block, this allows estimating the magnitude of the symmetry-allowed terms. Terms that were not present before block-diagonalization are called contributions from remote bands. For example, using the 8×8 Kane model, one can calculate the parameters γ_i that enter the 4×4 Luttinger Hamiltonian [Equation (6)] for the top of the valence band; because the model is isotropic, one gets $\gamma_2 = \gamma_3$. To estimate corrections due to the cubic symmetry, one needs to take more bands into account.

In addition to the crystal field, we also wish to consider electric fields that are applied externally or that result from charged impurities. Assuming that the corresponding potential $V(\mathbf{r})$ varies slowly on the scale of a lattice constant, we can apply the envelope function approximation (EFA), i.e., we replace the plain wave $e^{i\mathbf{k}\cdot\mathbf{r}}$ by a slowly varying envelope function $\psi(\mathbf{r})$. Evaluating matrix elements of V in the basis $\langle \mathbf{r} | \psi, \nu \rangle = \psi(\mathbf{r}) u_{\nu, \mathbf{k}=0}(\mathbf{r})$, the main contribution is diagonal with respect to the band index ν . However, because \mathbf{k} and $V(\mathbf{r})$ do not commute, off-diagonal elements (in ν) can arise in the Hamiltonian when expanding in \mathbf{k} , see e.g.

Equation (4). Magnetic fields can be included in a similar way, using the Perierls substitution $\hbar\mathbf{k} = -i\hbar\nabla - (e/c)\mathbf{A}$. Here, we use $e < 0$ for electrons and $e > 0$ for holes. Then, the components of \mathbf{k} no longer commute, $\mathbf{k} \times \mathbf{k} = i(e/\hbar c)\mathbf{B}$; this leads to Zeeman coupling, which is described by an effective g factor.

2.2 Effective Hamiltonian

The $\mathbf{k} \cdot \mathbf{p}$ method leads to high-dimensional Hamiltonians [Equation (5)], for example, an 8×8 matrix for the Kane model, thus further simplifications are desirable. For this, one can use time-independent degenerate perturbation theory and describe a subset of states (say, the lowest conduction band states) with an effective Hamiltonian. Löwdin partitioning is a straightforward and convenient method to implement such a perturbative expansion (Winkler, 2003); it is also known as Foldy-Wouthuysen transformation in the context of the Dirac equation and as Schrieffer-Wolf transformation in the context of the Anderson model. The idea is to find a unitary transformation e^{-S} (i.e., S is anti-Hermitian) such that the transformed Hamiltonian $e^{-S}He^S$ is block diagonal, i.e., contains no off-diagonal elements between the states we are interested in and any other states. This procedure assumes that the states of interest (e.g., the conduction band) are separated from the other states (all other bands) by an energy much larger than the Fermi energy. Then, because these off-diagonal elements are small, one can eliminate the off-diagonal blocks of $e^{-S}He^S$ order by order (or even exactly). In our example, the transformed Hamiltonian consists of one 2×2 and one 6×6 block. The smaller block describes the conduction band electrons—we can understand the two dimensions as (pseudo-) spin $\frac{1}{2}$. At the level of wave functions, the periodic part of the electron wave function at a given $\mathbf{k} \neq 0$ is mainly described by the conduction band Bloch function at $k = 0$, but also contains a small admixture from the valence band Bloch functions.

2.3 Intrinsic spin-orbit coupling

One generally distinguishes between intrinsic and extrinsic mechanisms of spin-orbit coupling; however, this classification is not unique across the literature. In this article, we classify it according to the individual terms of the effective Hamiltonians. Namely, we refer to the spin-orbit contributions to the Hamiltonian that depend on impurity potentials as *extrinsic*. The other spin-orbit contributions arise even in the absence of impurities and we call them *intrinsic*—we also call effects resulting from these contributions intrinsic, even if we must allow for a small concentration of impurities to make the theory of dc transport properties consistent.¹

For a (pseudo-) spin- $\frac{1}{2}$ system, the spin-orbit part of the intrinsic one-particle Hamiltonian has the general form H_{int} [Equation (3)]. In the following, we discuss the origin and the functional form of such spin-orbit fields. We focus on such spin- $\frac{1}{2}$

¹This is reminiscent of the definition of an “intrinsic semiconductor,” which is so pure that (at a sufficiently high temperature) the impurity contribution to the carrier density is negligible. The conductivity of such a sample is known as *intrinsic* conductivity (again, a finite transport lifetime τ is required to make the conductivity well-defined). At lower temperatures, the carrier density mainly results from the impurities and now one refers to *extrinsic* properties.

descriptions, because they are relevant for low-dimensional systems and are the basis of most theoretical works.

We first consider a n -doped bulk (3D) semiconductor and the effective Hamiltonian of conduction band electrons. III-V and II-VI semiconductors lack inversion symmetry and are available in two modifications: in cubic zinc blende or in hexagonal wurtzite structure. In zinc blende modification, the bulk inversion asymmetry (BIA) leads to the Dresselhaus term

$$H_{\text{D},3\text{d}} = \mathcal{B} k_x (k_y^2 - k_z^2) \sigma_x + \text{c.p.}, \quad (7)$$

where k_i are along the principal crystal axes. Here, c.p. stands for cyclic permutation of all indices, and the symmetrized product of the components k_i must be used if a magnetic field is applied. The Dresselhaus term originates from bands further away than the basic eight bands, and one finds the coupling constant in terms of the band parameters; when using the extended 14×14 Kane model its numerical value is $\mathcal{B} \approx 27 \text{ eV}\text{\AA}^3$, for both GaAs and InAs (Winkler, 2003).

When the electrons are confined to two dimensions, the expectation value of the Dresselhaus term along the confinement direction (that we always assume to be along [001]) should be taken, $\langle H_{\text{D},3\text{d}} \rangle$. While $\langle k_z \rangle = 0$, we see that the terms in $\langle k_z^2 \rangle \approx (\pi/d)^2$ are large for small confinement width d , thus the main BIA contribution becomes

$$H_\beta = \beta (k_x \sigma_x - k_y \sigma_y), \quad (8)$$

with $\beta \approx -\mathcal{B} (\pi/d)^2$. In addition to the k -linear term in Equation (8), there is also a k^3 -term,

$$H_{\text{D},2\text{d}} = \mathcal{B} k_x k_y (k_y \sigma_x - k_x \sigma_y), \quad (9)$$

which is small compared to H_β in the strong confinement (low carrier density) limit $\pi/d \gg k_{\text{F}}$, where k_{F} is the Fermi wave vector. Additionally, a spin-orbit coupling term arises if the confinement potential $V(z)$ along the z -direction is not symmetric, i.e., if there is a structure inversion asymmetry (SIA). Equation (4) provides an explicit connection between such a potential and spin-orbit coupling. Taking the expectation value $\langle H_{\text{ext}} \rangle$ along the z -direction and noting that the only contribution of the confinement field is $\propto \langle \nabla_z V \rangle$, one finds the Rashba Hamiltonian,

$$H_\alpha = \alpha (k_y \sigma_x - k_x \sigma_y), \quad (10)$$

corresponding to $\mathbf{b}(\mathbf{k}) = 2\alpha \hat{\mathbf{z}} \times \mathbf{k}$. More generally, for spinors with $J_z = \pm 1/2$, H_α is the only k -linear invariant of the group $C_{\infty v}$ that takes into account the confinement potential $V(z)$ but disregards the discrete symmetry of the crystal. The magnitude of the coupling constant α depends on the confining potential and it can be modified by applying an additional field via external gates. It also defines the spin-precession wave vector $k_\alpha = \alpha m/\hbar^2$. Finally, such a term H_α is also present for three-dimensional electrons in systems of hexagonal wurtzite structure (or in cubic systems with strain, see Sec. 2.5).

Next, we consider a p -doped three dimensional semiconductor, i.e., the $J = 3/2$ valence band, described by the four-dimensional Luttinger Hamiltonian. Remote bands lead to a BIA contribution to the Hamiltonian, which is given by Equation (7) after replacing σ_i by the angular momentum matrices J_i for spin $\frac{3}{2}$ and using a different coupling constant. If the system is reduced to two dimensions, size quantization lifts the fourfold degeneracy at $\mathbf{k} = \mathbf{0}$ and creates heavy-hole (HH) bands with $J_z = \pm 3/2$, and light-hole (LH) bands with $J_z = \pm 1/2$; for simplicity, we consider confinement along the [001] axis. Usually the HH bands are higher in energy, thus for small doping it is sufficient to consider only them. For spinors with $J_z = \pm 3/2$, the only invariant of the group $C_{\infty v}$ (again, we do not discuss invariants of discrete symmetries here) respecting time reversal symmetry is

$$H_{\alpha,h} = i\alpha_h (k_-^3 \sigma_+ - k_+^3 \sigma_-), \quad (11)$$

where $a_{\pm} \equiv a_x \pm ia_y$ for any a . As distinct from H_{α} [Equation (10)], the Rashba Hamiltonian for heavy holes is cubic in k , as it was discussed in (Winkler, 2000; Schliemann and Loss, 2005).

2.4 Extrinsic spin-orbit coupling

Electric fields due to impurities lead to extrinsic contributions of the spin-orbit coupling. Externally applied electrical fields lead to analogous contributions. To derive the dominant extrinsic term, it is sufficient to restrict ourselves to the simplest 8×8 Kane Hamiltonian; higher bands will give rise to small corrections. Using third-order perturbation theory and for conduction band electrons, we find H_{ext} as given in Equation (4), with (Nozières and Lewiner, 1973; Winkler, 2003)

$$\lambda \approx \frac{P^2}{3} \left[\frac{1}{E_0^2} - \frac{1}{(E_0 + \Delta_0)^2} \right], \quad (12)$$

where V is the potential due to impurities and an externally applied field. It is noteworthy that Equation (4) has the same analytical form as the vacuum spin-orbit coupling [Equation (1)]; this is because both the Dirac equation and the simplest Kane Hamiltonian have spherical symmetry and because both the Pauli equation and Equation (4) are obtained in a low-energy expansion. However, for $\Delta_0 > 0$ the coupling constant λ has the *opposite sign* as in vacuum.

One finds $\lambda \approx 5.3 \text{ \AA}^2$ for GaAs and $\lambda \approx 120 \text{ \AA}^2$ for InAs, i.e., spin-orbit coupling in n -GaAs is by six orders of magnitude stronger than in vacuum, and even larger for InAs due to its smaller gap. This enhancement of spin-orbit coupling is critical for developing large extrinsic spin currents. Furthermore, for a two-dimensional system, when considering V as averaged along the $\hat{\mathbf{z}}$ -direction, both ∇V and \mathbf{k} are in-plane, thus we have $H_{\text{ext,e}} = \lambda \sigma_z (\mathbf{k} \times \nabla V)_z$.

For a 3D hole system, we consider the $J = 3/2$ valence band. Then, the dominant extrinsic spin-orbit term in third order perturbation theory describing the valence band states is

$$H_{\text{ext,v}} = \lambda_v \mathbf{J} \cdot (\mathbf{k} \times \nabla V), \quad (13)$$

with $\lambda_v = -P^2/3E_0^2$, i.e., for GaAs $\lambda_v \approx -15 \text{ \AA}^2$ (Winkler, 2003). and has to be added to the Luttinger Hamiltonian H_L [Equation (6)]. When considering a two-dimensional hole system with HH-LH splitting, we can restrict Equation (13) to the heavy holes states, where $J_z = \pm 3/2$. Expressing this two-dimensional subspace in terms of a pseudo-spin $\frac{1}{2}$ leads to

$$H_{\text{ext},v} = -\frac{P^2}{2E_0^2} (\mathbf{k} \times \nabla V)_z \sigma_z. \quad (14)$$

Thus, the extrinsic spin-orbit interaction for two-dimensional heavy hole states has the same form as for two-dimensional electrons.

Finally we point out that extrinsic spin-orbit coupling arises because the long range Coulomb potential of the impurities does not commute with the intrinsic Hamiltonian of the hosting crystal. The extrinsic Hamiltonian H_{ext} [Equations (4) and (13)] is obtained in the framework of the EFA, which disregards short-range contributions of the spin-orbit coupling arising from the chemical properties of dopants. This is why the coupling λ depends only on the parameters of the perfect crystal lattice.

2.5 Strain

Non-hydrostatic strain reduces the symmetry of the system and in this way leads to additional spin-orbit terms in the Hamiltonian. In third order perturbation theory of the Kane Hamiltonian, the effective conduction-band Hamiltonian due to strain is dominated by

$$H_{\varepsilon,e} = \frac{-2C_2\Delta_0P}{3E_0(E_0 + \Delta_0)} \boldsymbol{\sigma} \cdot (\mathbf{k} \times \boldsymbol{\varepsilon}_s) \equiv \frac{1}{2}C_3 \boldsymbol{\sigma} \cdot (\mathbf{k} \times \boldsymbol{\varepsilon}_s), \quad (15)$$

where $\boldsymbol{\varepsilon}_s = (\varepsilon_{yz}, \varepsilon_{xz}, \varepsilon_{xy})$ describes the shear strain. Here, C_2 is the interband deformation-potential constant that arises in noncentrosymmetric semiconductors (Winkler, 2003; Trebin *et al.*, 1979). Note that Pikus and Titkov (1984) as well as Ivchenko and Pikus (1997) use the opposite sign in the definition of this constant, $C_2^{\text{PT/IP}} = -C_2$. Further, if a shear is applied such that only $\varepsilon_{xy} \neq 0$, Equation (15) has the same form as the Rashba Hamiltonian [Eq. (10)].

For three-dimensional $J = 3/2$ valence band states, the main strain contribution is (Pikus and Titkov, 1984)

$$H_{\varepsilon,v} = \frac{2C_2P}{3E_0} \mathbf{J} \cdot (\mathbf{k} \times \boldsymbol{\varepsilon}_s). \quad (16)$$

Note that when the system is confined to two dimensions, Equation (16) implies a k -linear spin-orbit contribution for heavy hole states due to strain, $(C_2P/E_0) (\mathbf{k} \times \boldsymbol{\varepsilon}_s)_z \sigma_z$. This linear term arises due to the low symmetry of the strained material, in contrast to the Rashba term [cf. Equation (11)], which is dominated by terms cubic in k and where the k -linear terms are numerically small (Winkler, 2003).

2.6 Anomalous velocity and coordinate

As a consequence of the spin-orbit interaction, velocity and coordinate operators are modified and become spin dependent—this will be important when considering currents. When an effective Hamiltonian is derived in perturbation theory, as explained in Sec. 2.2, a unitary transformation e^{-S} is applied. Thus, the coordinate operator $\mathbf{r} = i(\partial/\partial\mathbf{k})$ is also transformed, $\mathbf{r} \mapsto \tilde{\mathbf{r}} = e^{-S}\mathbf{r}e^S = \mathbf{r} + \delta\mathbf{r}$ and we call $\delta\mathbf{r}$ the anomalous coordinate. In particular, because S couples to spin, $\delta\mathbf{r}$ is spin-dependent. This correction $\delta\mathbf{r}$ is known as the Yafet term (Yafet, 1963); also, it can be expressed in terms of a Berry connection, $\langle u_{\nu',\mathbf{k}} | i\nabla_{\mathbf{k}} | u_{\nu,\mathbf{k}} \rangle$. In perturbation theory, one finds

$$\delta\mathbf{r}_{\text{SO},e} = \lambda(\boldsymbol{\sigma} \times \mathbf{k}), \quad (17)$$

$$\delta\mathbf{r}_{\text{SO},v} = \lambda_v(\mathbf{J} \times \mathbf{k}), \quad (18)$$

for conduction band electrons and for $J = 3/2$ heavy hole states, respectively. Note that coordinate operators no longer commute, $\mathbf{r} \times \mathbf{r} = i\lambda\boldsymbol{\sigma}$ and $\mathbf{r} \times \mathbf{r} = i\lambda_v\mathbf{J}$, resp. Finally, $\delta\mathbf{r}_{\text{SO}}$ leads to an extra term in the equations of motion that can be understood as anomalous velocity (Blount, 1962).

Formally, we can derive the anomalous velocity similarly to the coordinate, namely $\mathbf{v} \mapsto e^{-S}\mathbf{v}e^S = \mathbf{v}_0 + \delta\mathbf{v}$, where $\delta\mathbf{v}$ is the anomalous velocity and, for a parabolic band, $\mathbf{v}_0 = \hbar\mathbf{k}/m^*$. Alternatively, one can obtain the velocity operator from the Heisenberg equation, $\mathbf{v} = (i/\hbar)[H, \tilde{\mathbf{r}}]$. For $H = H_0 + H_{\text{SO}}$, where H_{SO} contains the (small) spin-orbit coupling, we get $\mathbf{v} = \mathbf{v}_0 + (i/\hbar)[H_{\text{SO}}, \mathbf{r}] + (i/\hbar)[H_0, \delta\mathbf{r}_{\text{SO}}]$. Thus, H_{SO} leads to an anomalous velocity because it does not commute with the unperturbed coordinate \mathbf{r} , and, additionally, the contribution from the anomalous coordinate $\delta\mathbf{r}_{\text{SO}}$ should also be taken into account, as it can be significant.

When the impurity potential V is included, the above argument remains the same, but now H_{SO} contains the extrinsic contribution as well. Note that for extrinsic spin-orbit $H_{\text{SO}} = H_{\text{ext},e}$ [Equation (4)] the commutator $[H_{\text{ext},e}, \mathbf{r}]$ and the anomalous coordinate $\delta\mathbf{r}_{\text{SO}}$ give equal contributions to $\delta\mathbf{v}$ (Nozières and Lewiner, 1973).

3 Mechanisms of spin transport

We now address how the microscopic mechanism of spin-orbit interaction, given by effective Hamiltonians, influences spin transport and accumulation. In the following, we assume a non-interacting system in the absence of a magnetic field. Because we ignore electron-electron interaction, we do not consider the spin-drag effect here (Hankiewicz and Vignale, 2006), which can lead to a suppression of spin transport at high temperatures, and suppression of spin-relaxation (Glazov and Ivchenko, 2002). We also restrict ourselves to Boltzmann transport and do not discuss the hopping regime (Entin-Wohlman *et al.*, 2005).

3.1 Intrinsic: spin precession

In a system with weak intrinsic spin-orbit coupling H_{int} [Equation (3)], consider a carrier with spin aligned along the spin-orbit field $\mathbf{b}(\mathbf{k})$. When an electrical field $\mathbf{E} = E\hat{\mathbf{x}}$ is applied, the particle is accelerated: $\dot{\mathbf{k}} = e\mathbf{E}/\hbar$ in lowest order in spin orbit-interaction; and its spin-orbit field changes: $\dot{\mathbf{b}} = (\partial\mathbf{b}/\partial k_x) eE/\hbar$. For a small acceleration, the spin follows adiabatically the direction of $\mathbf{b}(\mathbf{k})$. Additionally, there will be a non-adiabatic correction that can be derived as follows. Say, the direction of \mathbf{b} rotates in the xy plane (as it is the case for Rashba interaction H_α). Because the rotation frequency ω is the component of $\dot{\mathbf{b}}/b$ perpendicular to \mathbf{b} , it is $\omega = (\mathbf{b} \times \dot{\mathbf{b}})_z/b^2$. In the co-rotating frame, there is a field b along the x -axis and a field $\hbar\omega$ along the z -axis. As we are interested in the next-to-adiabatic correction, we assume that ω changes slowly and that the spin remains aligned along the total field in the rotating frame, thus it has a component $s_z \approx (\hbar/2)\hbar\omega/b$. Therefore the first non-adiabatic correction to the spin is $\delta\mathbf{s}(\mathbf{k}) = \hbar^2(\mathbf{b} \times \dot{\mathbf{b}})_z/2b^3$. In particular, the electrical field drives this spin precession (via $\dot{\mathbf{b}}$), leading to such out-of-plane component $\delta\mathbf{s}(\mathbf{k})$, which could be important in spin transport (Sinova *et al.*, 2004), see Sec. 4.3. However, when considering dc properties, one must be careful and also allow for impurities that decelerate the carriers to reach a steady state. In particular, if $\mathbf{b}(\mathbf{k})$ is linear in \mathbf{k} , it turns out that the deceleration at impurities cancels this spin precession, see Sec. 4.3.

3.2 Extrinsic: skew scattering

When a carrier scatters at an impurity potential V , because of the extrinsic spin-orbit interaction [Equations (4) and (14)] the scattering cross section depends on the spin state (Smit, 1958), see Fig. 2. This effect is known as Mott skew scattering (Mott and Massey, 1965) and was originally considered for high-energy electrons that are elastically scattered by an atom and that are described by the vacuum Hamiltonian, Equation (1). Skew scattering does not appear in the first order Born approximation, thus is at least of the order V^3 . For band electrons, skew scattering was originally considered as the origin of the anomalous Hall effect, see Sec. 4.4. As applied to spin Hall effect, the relevance of this extrinsic mechanism was recognized early on (D'yakonov and Perel', 1971; Hirsch, 1999; Zhang, 2000).

3.3 Extrinsic: side jump mechanism

The side jump mechanism (Berger, 1970) describes the lateral displacement of the wave function during the scattering event. (Such a displacement does not modify the skew scattering cross section introduced in Sec. 3.2, because it does not change the scattering angle measured at large distances.) The side-jump contribution is obtained when the anomalous velocity $\delta\mathbf{v}$ (see Sec. 2.6) is integrated over the duration of the scattering process. As indicated in Sec. 2.6, the anomalous coordinate for electrons [Equation (17)] leads to an anomalous velocity contribution $\lambda(\boldsymbol{\sigma} \times \dot{\mathbf{k}})$; and there is an equal term due to $(i/\hbar)[H_{\text{ext},e}, \mathbf{r}]$. For impurity scattering with momentum transfer $\delta\mathbf{k}$, this results in a total lateral displacement $2\lambda(\boldsymbol{\sigma} \times \delta\mathbf{k})$ [and

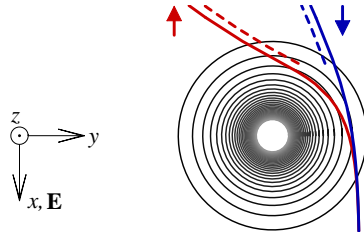


Figure 2: Spin-dependent scattering of electrons at an attractive impurity. We show the classical trajectories (solid lines), for a screened Coulomb potential and for strongly exaggerated extrinsic spin-orbit coupling [using Equation (4) with $\lambda = \lambda > 0$] and with spin quantization axis perpendicular to the plane. The skew-scattering current results from different scattering angles for spin- \uparrow and spin- \downarrow electrons and leads to a positive spin Hall conductivity, $\sigma_{SS}^{\text{SH}} = -j_{SS,y}^z/E_x > 0$. The dashed lines show the horizontal displacement due to the side jump effect, contributing to the spin current with opposite sign.

analogously for holes, using Equation (18)]. When also the effects of the anomalous velocity due to an applied electrical field is considered, the side-jump contribution to spin-transport becomes a subtle issue, for a detailed analysis and intuitive description see (Nozières and Lewiner, 1973). Because the side jump mechanism is not contained in the Boltzmann approach, in such a framework it needs to be evaluated separately. The side jump contribution can be found using the Kubo formula and diagrammatic approaches; see (Lewiner *et al.*, 1973; Crépieux and Bruno, 2001; Tse and Das Sarma, 2006).

3.4 Kinetic equation

We consider the Hamiltonian H_{eff} [Equation (2)] containing both intrinsic (H_{int}) and extrinsic (H_{ext}) spin-orbit contributions, and with V that describes the electrical field \mathbf{E} and the impurity potential V_i . For a homogeneous system of non-interacting particles, one can derive the kinetic equation (Khaetskii, 2006; Shytov *et al.*, 2006)

$$\frac{\partial \hat{f}}{\partial t} + \frac{1}{\hbar} \boldsymbol{\sigma} \cdot (\mathbf{b} \times \mathbf{f}) + e\mathbf{E} \cdot \frac{1}{\hbar} \frac{\partial \hat{f}_0}{\partial \mathbf{k}} = \left(\frac{\partial \hat{f}}{\partial t} \right)_{\text{coll}}, \quad (19)$$

i.e., a spin-dependent Boltzmann equation, where the distribution function is written as a 2×2 spin matrix $\hat{f} = \hat{f}_0(\mathbf{k}) + \frac{1}{2}n(\mathbf{k}) \mathbb{1} + \mathbf{f}(\mathbf{k}) \cdot \boldsymbol{\sigma}$, with equilibrium distribution function \hat{f}_0 . Here, n is the excess particle density and \mathbf{f} describes the spin polarization density. Formally, the Boltzmann equation is obtained by an expansion in $1/k_F \ell$, where ℓ is the mean free path, i.e., it is applicable for dilute impurities. Traditionally, the Boltzmann equation describes the distribution function $n(\mathbf{k})$, which is the *probability* density of a state \mathbf{k} to be occupied—in contrast, here it describes $\hat{f}(\mathbf{k})$, which corresponds to the 2×2 *density matrix* for a spin- $\frac{1}{2}$ particle.

All terms on the l.h.s. of Equation (19) arise in the absence of impurities. The first term is the derivative of \hat{f} with respect to its explicit time-dependence. The second term describes the spin precession; it is obtained from the Heisenberg equation, $\mathbf{f} \cdot \dot{\boldsymbol{\sigma}} = \mathbf{f} \cdot (i/\hbar) [-\frac{1}{2}\mathbf{b}(\mathbf{k}) \cdot \boldsymbol{\sigma}, \boldsymbol{\sigma}]$. The third term is the driving term due to the electrical field, given in lowest order of \mathbf{E} . Finally, for inhomogeneous particle and spin distributions, the term $\mathbf{v} \cdot \nabla \hat{f}$ has to be added to the l.h.s.

The r.h.s. of the Boltzmann equation [Equation (19)] is the collision term, symbolically given by

$$\left(\frac{\partial \hat{f}(\mathbf{k})}{\partial t} \right)_{\text{coll}} = n_i v \sum_{\mathbf{k}'; \epsilon'=\epsilon} \frac{d\vec{\sigma}}{d\Omega} [\hat{f}(\mathbf{k}') - \hat{f}(\mathbf{k})], \quad (20)$$

Here, n_i is the impurity density and we only consider elastic scattering $\mathbf{k} \rightarrow \mathbf{k}'$ and $\mathbf{k}' \rightarrow \mathbf{k}$. The scattering cross section tensor $d\vec{\sigma}/d\Omega$ and the summation over final states \mathbf{k}' are spin-dependent because (i) the extrinsic interaction H_{ext} leads to skew-scattering, (ii) the intrinsic spin-orbit Hamiltonian H_{int} induces a spin-dependent density of states, and (iii) H_{int} causes spin-dependent momentum transfer—in general, the spin dependence of scattering is rather complex. The description of scattering is simplified for weak spin orbit coupling, as the collision term can be expanded in spin-orbit coupling, and we can discuss the individual corrections separately. Note that the Boltzmann equation does not include the side-jump effect (cf. Sec. 3.3), which is of higher order in $1/k_F \ell$.

When considering only spin-orbit coupling due to H_{ext} , the collision term including skew scattering for a central symmetric impurity potential is (Engel *et al.*, 2005)

$$\left(\frac{\partial \hat{f}(\mathbf{k})}{\partial t} \right)_{\text{coll}} = n_i v_\epsilon \int d\Omega(\mathbf{k}') \left\{ I(\vartheta) [\hat{f}(\mathbf{k}') - \hat{f}(\mathbf{k})] + \frac{1}{2} I(\vartheta) S(\vartheta) \boldsymbol{\sigma} \cdot \mathbf{m} [n(\mathbf{k}) + n(\mathbf{k}')] \right\} \quad (21)$$

where $\mathbf{m} = \mathbf{k}' \times \mathbf{k} / |\mathbf{k}' \times \mathbf{k}|$ is the unit vector normal to the scattering plane and $\vartheta = \vartheta_{\mathbf{k}\mathbf{k}'}$ is the angle between \mathbf{k}' and \mathbf{k} . The coefficient $I(\vartheta)$ is the spin-independent part of the scattering cross section, while $S(\vartheta)$ is the so-called Sherman function (Mott and Massey, 1965; Motz *et al.*, 1964; Huang *et al.*, 2003), describing the polarization of outgoing particles (which is normal to the scattering plane) scattered into direction \mathbf{k} from an unpolarized incoming beam of momentum \mathbf{k}' . Note that IS , as mentioned earlier in Sec. 3.2, vanishes in first-order Born approximation; the lowest term is $\propto V^3$. Also, S is proportional to spin-orbit coupling, this is why in the second term in Equation (21), only the spin-independent part of \hat{f} , $\frac{1}{2}n$, is retained.

So far, we considered the distribution function $\hat{f}(\mathbf{k})$ as density in \mathbf{k} -space. In the presence of intrinsic spin-orbit interaction, the energy spectrum contains two branches: for a given \mathbf{k} , there are two energies, split by the intrinsic field $\mathbf{b}(\mathbf{k})$. Thus, for elastic scattering, energy is conserved but $|\mathbf{k}|$ is not. It is now more convenient to choose a distribution as function of energy ϵ and direction φ in \mathbf{k} -space. Namely, the distributions $\Phi_c(\varphi, \epsilon)$ and $\Phi(\varphi, \epsilon)$ are given by the distributions $n(\mathbf{k})$ and $\mathbf{f}(\mathbf{k})$ integrated over a small cone in \mathbf{k} -space, and can again be written as matrix $\hat{\Phi}(\varphi, \epsilon)$.

Note that $\hat{\Phi}$ contains the spin-dependent DOS. We now consider a two-dimensional system, $\mathbf{k} = (k \cos \varphi, k \sin \varphi)$, and assume that the spectrum ϵ_k in the absence of spin-orbit interaction is isotropic [cf. Equation (2)], and we define k_ϵ such that $\epsilon_{k_\epsilon} = \epsilon$ and define $v_\epsilon = \epsilon'_{k_\epsilon}/\hbar$. For $\mathbf{E} = E\hat{\mathbf{x}}$ and for $b \ll E_F$, the kinetic equation becomes (Shytov *et al.*, 2006)

$$\frac{\partial \hat{\Phi}}{\partial t} + \boldsymbol{\sigma} \cdot \left[\frac{\mathbf{b} \times \boldsymbol{\Phi}}{\hbar} - \frac{\Phi_c}{4\hbar^2 v_\epsilon} \mathbf{b} \times \frac{\partial \mathbf{b}}{\partial k} \right] + \frac{eE}{(2\pi)^2} \frac{\partial f_0}{\partial \epsilon} \left[\frac{k_x}{\hbar} + \frac{1}{2\hbar^2 v_\epsilon} \frac{\partial}{\partial \varphi} (\mathbf{b} \cdot \boldsymbol{\sigma} \sin \varphi) \right] = \left(\frac{\partial \hat{\Phi}}{\partial t} \right)_{\text{coll}}, \quad (22)$$

where f_0 is the Fermi distribution function and \mathbf{b} is evaluated for $|\mathbf{k}| = k_\epsilon$.

Now, considering only H_{int} , the collision integral can be found in a Golden Rule approximation (Shytov *et al.*, 2006),

$$\begin{aligned} \left(\frac{\partial \hat{\Phi}(\varphi, \epsilon)}{\partial t} \right)_{\text{coll}} &= \int_0^{2\pi} d\varphi' K(\vartheta) \left[\hat{\Phi}(\varphi') - \hat{\Phi}(\varphi) \right] \\ &+ \int_0^{2\pi} d\varphi' \boldsymbol{\sigma} \cdot [\mathbf{M}(\varphi, \varphi') \Phi_c(\varphi') - \mathbf{M}(\varphi', \varphi) \Phi_c(\varphi)]. \end{aligned} \quad (23)$$

Here, the first term describes the spin-independent scattering, with $K(\vartheta) = K(\varphi' - \varphi) = W(q) k_\epsilon / 2\pi \hbar^2 v_\epsilon$ and $q = 2k_\epsilon \sin(|\vartheta|/2)$. The factor $W(q) = \langle |V_i(\mathbf{q})|^2 \rangle$ does not depend on the direction of the momentum transfer \mathbf{q} because the problem is isotropic (while of course the individual scattering event is anisotropic, i.e., depends on the scattering angle ϑ). This spin-independent term coincides with first term of Equation (21), with $K(\vartheta) = n_i v_\epsilon I(\vartheta)$, and should only be included once. The second term in Equation (23) is given in first order in the intrinsic spin-orbit interaction \mathbf{b} and contains the kernel (Shytov *et al.*, 2006)

$$\mathbf{M}(\varphi, \varphi') = \frac{v_\epsilon}{4k_\epsilon} K(\vartheta) \frac{\partial}{\partial \epsilon} \left[\frac{k_\epsilon \mathbf{b}(\varphi)}{v_\epsilon} \right] + \frac{\mathbf{b}(\varphi) + \mathbf{b}(\varphi')}{4\hbar k_\epsilon v_\epsilon} \frac{\partial K(\vartheta)}{\partial \vartheta} \tan \frac{\vartheta}{2}, \quad (24)$$

where the first term results from the spin-dependent DOS of the outgoing wave. The second term in \mathbf{M} arises, because for a given energy ϵ , $|\mathbf{k}|$ depends on the spin state. Thus the incoming and outgoing states can have different momenta, leading to spin-dependent corrections to q .

For a very smooth scattering potential such that typically $q < b/v_F$, the spin motion is adiabatic and should be treated differently (Govorov *et al.*, 2004; Khaetskii, 2006).

3.5 Diffusion equation

A spin diffusion equation can be derived, starting from the Boltzmann equation, for a dirty system when the spin relaxation time τ_s is much longer than the momentum relaxation time τ , i.e., $\tau_s \gg \tau$. It describes the carrier density $N(\mathbf{r})$ and spin polarization density $\mathbf{s}(\mathbf{r})$; say, s_z is the excess density of particles polarized along $\hat{\mathbf{z}}$. For conduction band electrons, the (pseudo-) spin density is $\mathbf{S} = (\hbar/2)\mathbf{s}$. The diffusion

equation is simpler to solve than the kinetic equation (19), as the dependence on \mathbf{k} is integrated out. Also, it is usually sufficient to know \mathbf{s} , because it is an experimentally accessible quantity, while $\hat{f}(\mathbf{k})$ is not directly accessible, cf. Secs. 4.2 and 4.5 below. For a two-dimensional system with Rashba spin-orbit interaction H_α [Equation (10)], the diffusion equation is (Burkov *et al.*, 2004; Mishchenko *et al.*, 2004)

$$\dot{N} = D\nabla^2 (N + \rho_0 V_E) + \Gamma_{\text{sc}} (\nabla \times \mathbf{s})_z, \quad (25)$$

$$\dot{s}_i = D\nabla^2 s_i - \tau_i^{-1} s_i + \Gamma_{\text{ss}} [(\hat{\mathbf{z}} \times \nabla) \times \mathbf{s}]_i + \Gamma_{\text{sc}} (\hat{\mathbf{z}} \times \nabla)_i (N + \rho_0 V_E), \quad (26)$$

with diffusion constant $D = \frac{1}{2}v_{\text{F}}^2\tau$, anisotropic Dyakonov-Perel (1972) spin relaxation rates $\tau_x^{-1} = \tau_y^{-1} = \tau_\perp^{-1} = 2\tau(\alpha k_{\text{F}}/\hbar)^2$ and $\tau_z^{-1} = 2\tau_\perp^{-1}$, spin-charge coupling $\Gamma_{\text{sc}} = -2\alpha(\alpha k_{\text{F}}\tau)^2/\hbar^3$, spin-spin coupling $\Gamma_{\text{ss}} = 4\alpha E_{\text{F}}\tau/\hbar^2$, density of states $\rho_0 = m/\pi\hbar^2$, and potential energy V_E of a carrier in the electrical field. The charge current is

$$\mathbf{J}^{\text{c}} = -D\nabla(N + \rho_0 V_E) + \Gamma_{\text{sc}} \hat{\mathbf{z}} \times \mathbf{s}. \quad (27)$$

Further, Mal'shukov *et al.* (2005) derived diffusion equations for two-dimensional electrons with the Dresselhaus Hamiltonian $H_{\text{D},2\text{d}}$ [Equation (9)].

The boundary conditions of the diffusion equation for a system with spin-orbit interaction are not trivial and one expects that they depend on the microscopic properties of the boundaries. Although a number of papers have been written about the correct boundary conditions corresponding to various physical circumstances, there is currently still controversy about this issue (Govorov *et al.*, 2004; Mal'shukov *et al.*, 2005; Adagideli and Bauer, 2005; Galitski *et al.*, 2006; Bleibaum, 2006). Depending on the particular boundary condition, there may or may not be an s_z spin accumulation near the boundary of a 2D system, see Sec. 4.5. Somewhat related to these question, Shekhter *et al.* (2005) considered the boundary between a diffusive and ballistic system and allowed for spin-dependent scattering at the boundary, resulting from a spatially dependent Rashba Hamiltonian H_α .

4 Electrically induced spin polarization and spin transport

4.1 Spin current and spin Hall conductivity

In this article, we define the spin current in a homogeneous system with density n as

$$j_k^i \equiv \frac{1}{2} n \langle \sigma_i v_k + v_k \sigma_i \rangle, \quad (28)$$

where $\langle \cdot \rangle$ is the expectation value of single-particle operators and with $\langle 1 \rangle = 1$. Thus, the spin current is defined as the difference of the particle currents densities (measured in numbers of particles) for carriers with opposite spins. This is in accordance with many studies (Murakami *et al.*, 2003; Sinova *et al.*, 2004; Sinova *et al.*, 2006),

where a definition as in Equation (28) was chosen, up to numerical prefactors. In many definitions, an additional prefactor of $\frac{1}{2}$ is used, which results from $\hbar/2$ angular momentum per electron spin and setting $\hbar = 1$. With the same argument, for the HH band, sometimes a prefactor $3/2$ is used; but sometimes only a factor $\frac{1}{2}$ is used to have the same definition of \mathbf{j}^μ for electrons and holes. Furthermore, the r.h.s. of Equation (28) is sometimes multiplied by the charge e to obtain the same units for charge and for spin currents. In particular, this means that the sign of the definition of \mathbf{j}^μ may change if $e < 0$ for electrons is taken.

Next, we define the spin Hall conductivity

$$\sigma^{\text{SH}} \equiv -j_y^z/E_x, \quad (29)$$

where j_y^z is the spin current density resulting from a small applied electrical field E_x . The negative sign in Equation (29) results from writing a formal similar definition for σ^{SH} as for the charge conductivity σ_{xy} ; however, sometimes a definition with an opposite sign for σ^{SH} is used.

These various prefactors are only some technicality—the main question is whether defining j_k^i as in Equation (28) makes sense. To describe spin transport it sounds attractive to find a scheme similar to the charge transport theory. Because of charge conservation, charge densities ρ^c and charge currents \mathbf{j}^c satisfy the continuity equation $\dot{\rho}^c + \text{div } \mathbf{j}^c = 0$. For spin transport, we can consider the spin density S_i instead of ρ^c . Mott’s (1936) two-channel model of electron transport in ferromagnetic metals is based on independent and conserved currents of up- and down-spin electrons, and \mathbf{S} and j_k^i obey a continuity equation. The Definition (28) is the natural generalization of Mott’s model; however, spin-orbit coupling violates spin conservation, and the continuity equation for spin densities and currents does not hold. In this article, we will still use Equation (28) as definition of the spin current, as it is widely used, but we remain aware of its limitations. Despite the fact that it cannot be directly related to spin accumulation, it is a useful model quantity to compare the effect of different spin-orbit coupling mechanisms. While the continuity equation does not hold, one can, for a concrete Hamiltonian, evaluate source terms arising on the r.h.s. (Burkov *et al.*, 2004; Erlingsson *et al.*, 2005), which is often termed as torque (Culcer *et al.*, 2004).

Other definitions of spin currents have also been proposed. Zhang and Yang (2005) analyzed the current of the total angular momentum $L_z + S_z$ and argued that it vanishes for the Rashba Hamiltonian H_α in the absence of impurities (due to the rotational invariance of H_α) and that thus the impurity scattering would determine angular momentum currents. Shi *et al.* (2006) discussed spin currents, introducing a definition that is not proportional to our j_k^i , but is given as time-derivative of the “spin displacement” $S_i(\mathbf{r}) r_k$. A somewhat related definition was used by Bryksin and Kleinert (2006), who found that such spin currents diverge when the frequency $\omega \rightarrow 0$.

4.2 Spin polarization

In experiments, the spin polarization can be detected optically (Meier and Zakharchenya, 1984). Electrically induced polarizations were inferred from measure-

ments of the Kerr rotation, where the polarization of a linearly polarized beam of light rotates when the beam is reflected at a spin-polarized sample (Kato *et al.*, 2004b; Sih *et al.*, 2005). Alternatively, the circular polarization of the recombination light at a p - n junction can be used to determine the initial polarization of the carriers (Wunderlich *et al.*, 2005). Finally, the inverse effect, the photo-galvanic effect, can be observed, where a spin polarization is produced by polarized light and the induced electrical current is detected (Ganichev and Prettl, 2003).

In the bulk of a two- or three-dimensional sample, spin polarizations arise because an electrical field shifts the Fermi sea; $\langle \mathbf{k} \rangle = e\mathbf{E}\tau/\hbar$ for small E and with transport lifetime τ . This implies that due to intrinsic terms, there is on average a finite spin-orbit field, $\langle \mathbf{b}(\mathbf{k}) \rangle$. This leads to a bulk spin polarization, which, in simple cases, is aligned along $\langle \mathbf{b} \rangle$ (Ivchenko and Pikus, 1978; Vas’ko and Prima, 1979; Levitov *et al.*, 1985; Edelstein, 1990; Aronov *et al.*, 1991). Such a polarization was observed experimentally in two-dimensional GaAs hole systems: Silov *et al.* (2004) used a (001)-surface and detected the polarization of the photoluminescence from the side of the cleaved sample, while Ganichev *et al.* (2006) used samples of low crystallographic symmetry and detected the polarization along the growth direction. Furthermore, in the presence of anisotropic scattering (see Sec. 3.4), a magnetic field \mathbf{B} can lead to polarization perpendicular to both $\langle \mathbf{b} \rangle$ and \mathbf{B} (Engel *et al.*, 2006)—such a perpendicular polarization was already observed by Kato *et al.* (2004a).

4.3 Spin currents in bulk

The bulk spin current j_k^i was analyzed for many different spin-orbit Hamiltonians. For a two-dimensional electron system, the intrinsic effect of the Rashba coupling H_α lead to some debates. Because j_k^i is invariant under time reversal, it is allowed to be finite in equilibrium. Indeed, such equilibrium spin currents are predicted theoretically, however, they are of order α^3 and usually small (Rashba, 2003).

Now we discuss bulk spin currents driven by an external electrical field for systems with either intrinsic or extrinsic spin-orbit interaction. We do not discuss the more complicated case when both terms are present.

When an electrical field is applied and the electrons are accelerated, the precession described in Sec. 3.1 was considered. Because the initial spin density for a given direction of \mathbf{k} is proportional to α , but the non-adiabatic correction is proportional to $1/\alpha$, the spin-orbit coupling constant cancels. Initially, it was believed that a small concentration of impurities has no effect and a “universal” spin Hall conductivity $\sigma^{\text{SH}} = e/4\pi\hbar$ was predicted (Sinova *et al.*, 2004). However, it turns out that when the impurities are properly taken into account, the vertex correction cancels the bubble term, see Fig. 3. Thus, the dc conductivity σ^{SH} vanishes (Inoue *et al.*, 2004; Raimondi and Schwab, 2005),

$$\sigma^{\text{SH}} = 0, \tag{30}$$

which was confirmed in numerical calculations (Sheng, Sheng, Weng and Haldane, 2005). Only when the ac conductivity $\sigma^{\text{SH}}(\omega)$ is considered, in the regime $1/\tau \ll \omega \ll b/\hbar$ the universal value is recovered (Mishchenko *et al.*, 2004).

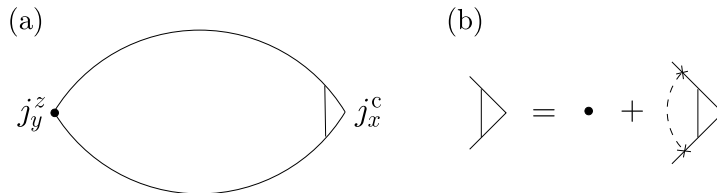


Figure 3: Diagram for spin Hall conductivity. The Kubo formula for σ^{SH} is proportional to $\text{Tr} \langle\langle j_y^z G_R j_x^c G_A \rangle\rangle$, with charge current operator j_x^c and retarded and advanced Green's functions $G_{R/A}$, and where $\langle\langle \cdot \rangle\rangle$ includes averaging over impurity configuration. In lowest order in $1/k_F \ell$, we can neglect crossed impurity lines and σ^{SH} is given by the diagram shown in (a). Here, the full lines symbolize the renormalized Green's functions including self-energy. In (b), the vertex renormalization due to impurity scatterings (connected by dashed line) is defined recursively. When only the first term of (b) is taken, we get the bubble contribution to σ^{SH} ; when all terms are summed, this leads to the additional (ladder) vertex correction.

That there are no bulk spin Hall currents can be understood by the following argument due to Dimitrova (2005). Using the Heisenberg equation and for parabolic bands, one finds the identity $d\sigma_y/dt = -(m\alpha/\hbar^2)(\sigma_z v_y + v_y \sigma_z)$ for single particle operators (Burkov *et al.*, 2004; Erlingsson *et al.*, 2005). For a homogeneous system, one then takes the expectation value of this identity and finds that $j_y^z \propto dS_z/dt$. When we consider dc properties, we must assume that the system is in a stationary state (i.e., we need impurity scattering). Then, the spin polarization S_z is constant and thus $j_y^z = 0$. These arguments, as well as spin current cancellation in a magnetic field in absence of scatterers (Rashba, 2004) shows that the cancellation is an intrinsic property of the free electron Hamiltonian H_α and is not related to any specific property of the scatterers. Furthermore, Chalaev and Loss (2005) find that the weak localization contribution to j_y^z vanishes, and show more generally that j_y^z vanishes even if both H_α and H_β are present. Grimaldi *et al.* (2006) find vanishing j_y^z for arbitrary values of $\alpha k_F/E_F$.

This cancellation is special to k -linear spin-orbit interaction (for nonparabolic bands, there can be a small finite contribution, proportional to α^2 (Krotkov and Das Sarma, 2006)). For example, for two-dimensional hole systems, the coupling $H_{\alpha,h}$ is cubic in k [Equation (11)]. Then, if isotropic scattering is assumed, the vertex correction vanishes, and a ‘‘universal’’ value $\sigma^{\text{SH}} = 3e/4\pi\hbar$ is found in the clean limit $b\tau \gg \hbar$ (Murakami, 2004; Schliemann and Loss, 2005). Quite generally, for a 2D system where the spin-orbit field $\mathbf{b}(\mathbf{k})$ winds $N \neq 1$ times around a circle in the xy plane when \mathbf{k} moves once around the Fermi circle (i.e., $N = 3$ for $H_{\alpha,h}$), a universal value

$$\sigma^{\text{SH}} = \frac{eN}{4\pi\hbar} \quad (31)$$

is found in the clean limit and for isotropic scattering (Shytov *et al.*, 2006; Khaetskii, 2006).

Also for the k^3 -Dresselhaus couplings, $H_{D,3d}$ and $H_{D,2d}$ [Equations (8) and (9)], the vertex corrections vanish for isotropic scattering. This leads to a finite spin Hall conductivity for two dimensional systems when $H_{D,2d}$ is considered (Mal'shukov and Chao, 2005). Similarly, σ^{SH} is finite for $H_{D,3d}$ (Bernevig and Zhang, 2004).

The results cited above are only valid for isotropic scattering [except Equation (30), which hold more generally]. Recently, more general descriptions using kinetic equation (cf. Sec. 3.4) allowed to include arbitrary angular dependence of impurity scattering (Shytov *et al.*, 2006; Khaetskii, 2006). It turns out that σ^{SH} significantly depends on the shape of the scattering potential and does not have a simple form in general. For example, in the clean limit $b\tau \gg \hbar$ and in the regime of small angle scattering (but still for a typical momentum transfer $q > b/v_F$, i.e., not too small angles), one finds

$$\sigma^{\text{SH}} = -\frac{eN}{2\pi\hbar} \left(\frac{N^2 - 1}{N^2 + 1} \right) (\tilde{N} - \zeta - 2) \quad (32)$$

where ζ describes the non-parabolicity of the band, $v_\epsilon \propto k_\epsilon^{1+\zeta}$, and for $|\mathbf{b}| \propto k^{\tilde{N}}$ (Shytov *et al.*, 2006). For example, taking $\zeta = 0$ and $H_{\alpha,h}$, with $N = \tilde{N} = 3$, we see that the sign of σ^{SH} in Equation [Equation (32)] is *opposite* to the case of isotropic scattering [Equation (31)]. Similarly, Liu and Lei (2005) found in a numerical study of system with spin-orbit coupling $H_{\alpha,h}$ that σ^{SH} strongly depends on the type of the scattering potential. Therefore, the spin Hall conductivity is not a universal quantity, as its numerical prefactor and its sign depend on sample parameters. On the other hand, for clean systems with $N \neq 1$, the order of magnitude is consistently $|\sigma^{\text{SH}}| \sim e/4\pi\hbar$.

The above results are valid for weak spin orbit coupling, $k_\alpha \ll k_F$. Conversely, there are also materials with strong spin-orbit coupling, as it was recently found in Bi/Ag (111) and Pb/Ag (111) surface alloys (Ast *et al.*, 2005). This motivated Grimaldi *et al.* (2006) to generalize the theory; however, relying on an extensive numerical procedure.

The extrinsic contribution $H_{\text{ext},e}$ for electrons also leads to spin currents (D'yakonov and Perel', 1971; Hirsch, 1999). These currents are often evaluated only for isotropic impurity scattering (Zhang, 2000; Shchelushkin and Brataas, 2005). Assuming absence of intrinsic spin-orbit interaction, for arbitrary angular dependence of scattering, the extrinsic spin Hall conductivity equals (Engel *et al.*, 2005)

$$\sigma^{\text{SH}} = -\frac{\gamma}{2e} \sigma_{xx} + 2n\lambda \frac{e}{\hbar}, \quad (33)$$

where the first term is due to skew scattering (see Sec. 3.2). The second term due to the side-jump mechanism (Sec. 3.3); as this mechanism goes beyond transport equation, this term has to be evaluated separately. Here, σ_{xx} is the electrical conductivity and we defined the transport skewness

$$\gamma = \frac{\int d\Omega I(\vartheta) S(\vartheta) \sin \vartheta}{\int d\Omega I(\vartheta) (1 - \cos \vartheta)} \quad (34)$$

that depends on the structure of the scattering center and on the Fermi energy, and I , S are defined below Equation (21). For screened Coulomb scatterers, Equation (33) can be evaluated without any free parameters (Engel *et al.*, 2005) and the resulting absolute value of spin current is in quantitative agreement (within error bars) with the observation by Kato *et al.* (2004b) in GaAs and seems comparable with the data by Stern *et al.* (2006) in ZnSe—implying that the observed spin currents are due to the extrinsic effect. Note that in Equation (33) the skew scattering and the side jump contributions have opposite signs. The skew scattering term dominates in standard transport theory where one expands in $\hbar/E\tau$ where E is a typical electron energy; however, for dirty samples both terms can be of comparable magnitude. Stern *et al.* (2006) found that the measured σ^{SH} in ZnSe has the sign of the skew scattering contribution and that the same is likely to be the case for the σ^{SH} observed by Kato *et al.* (2004b). Finally, assuming short-range scatterers, Tse and Das Sarma (2006) find the same order of magnitude for spin currents.

Remarkably, despite the fact that the side jump term in Equation (33) was derived by including electron dynamics during the scattering event, it does not contain any factors related to the scattering probability—it only depends on the coupling constant λ , which is an intrinsic property of the material and is directly related to a Berry connection through the spin-orbit contribution to the operator of electron coordinate, cf. Sec. 2.6. Thus, while in this review and commonly in the literature the side-jump contribution is considered as extrinsic, it is clear that the distinction between intrinsic and extrinsic is somewhat arbitrary.

4.4 Anomalous Hall effect and its relation to spin Hall effect

In the anomalous Hall effect (AHE), equilibrium polarization of a ferromagnet combined with spin-orbit interaction leads to electrical Hall currents transverse to an applied field. The theory of AHE has a long history and reveals many problems typical of spin transport in media with spin-orbit coupling, including the competing mechanisms of spin-orbit scattering by impurities and the role of intrinsic spin precession; for reviews see (Nozières and Lewiner, 1973; Crépieux and Bruno, 2001; Nagaosa, 2006). For non-interacting electrons and negligible spin relaxation, AHE and SHE are closely related; this is true for extrinsic spin-orbit interaction because λ is small and spin relaxation is of order λ^2 (Elliott, 1954; Yafet, 1963). In the SHE, we can decompose the spin currents \mathbf{j}^μ as a difference in particle currents of two spin species with polarizations $\pm\hat{\mathbf{e}}_\mu$. Regarding these species separately, each carries the anomalous Hall current $\mathbf{J}_{\text{AH}}^{\uparrow,\downarrow}$ of a system with spins fully aligned along the $\pm\hat{\mathbf{e}}_\mu$ direction and with density $n_{\text{AH}} = \frac{1}{2}n$, because we consider the SHE in non-magnetic media, where electrons are unpolarized in equilibrium. We can express the spin Hall current as (Engel *et al.*, 2005)

$$\mathbf{j}_{\text{SH}}^\mu = e^{-1} \left(\mathbf{J}_{\text{AH}}^\uparrow - \mathbf{J}_{\text{AH}}^\downarrow \right). \quad (35)$$

This relation allows to make use of the extensive literature on the AHE to gain further insights into mechanisms of the SHE, at least on its extrinsic part.

4.5 Spin accumulation and transport at boundaries

For only extrinsic spin-orbit coupling, because the spin relaxation is negligible for small λ , the spin is almost a conserved quantity and thus spin density and spin current satisfy a continuity equation with a small relaxation term. In this case, bulk spin currents will produce a spin polarization at the edge of the sample, i.e., spin currents and spin accumulation are directly related (D'yakonov and Perel', 1971; Hirsch, 1999; Zhang, 2000), the edge polarization at a $y = 0$ edge is $S_z = (\hbar/2) s_z = (\hbar/2) \sqrt{\tau_s/D_s} j_y^z$, with spin relaxation time τ_s and spin-diffusion coefficient D_s (which is identical to the electron diffusion coefficient D in the absence of electron-electron interaction).

For intrinsic spin-orbit interaction, however, it is not known whether any general relation between bulk currents and spin accumulation exists—but the spin accumulation was studied explicitly. Adagideli and Bauer (2005) considered a two-dimensional system with Rashba coupling H_α . Identifying the transverse edges of the sample as reservoirs without spin-orbit coupling, they argued that $s_i = 0$ at the boundary (see Sec. 3.5 for a discussion of boundary conditions). If an electrical field is applied along the x -direction, although there are no bulk spin currents j_y^z , still a spin accumulation $s_z(y)$ is found near a transverse edge and spin currents $j_k^i(y)$ also develop near them. The spin polarization $s_z(y)$ weakly oscillates and decays at the spin precession length $k_\alpha^{-1} = \hbar^2/m\alpha$, which is about the Dyakonov-Perel spin diffusion length $\sqrt{D_s\tau_s}$. Using similar boundary conditions written in terms of spin relaxation at the transverse edges, this polarization can be interpreted (Rashba, 2006) as the bulk spin polarization s_y (cf. Sec. 4.2) that is rotated out of the xy plane. Similar results were found using the boundary condition of Galitski *et al.* (2006) at a reflecting edge. However, as mentioned in Sec. 3.5, there is controversy about the correct boundary conditions. For example, Mal'shukov *et al.* (2005) proposed different boundary conditions and found that there is no spin accumulation near a reflecting edge. On the other hand, they did find such an accumulation when the Hamiltonian $H_{\text{int}} = H_\beta + H_{D,2d}$ is considered instead of H_α .

In the opposite limit of ballistic transport and near a sharp specular edge, Usaj and Balseiro (2005) have found spin magnetization due to H_α that oscillates rapidly with a period of k_F^{-1} and shows beating on a length scale of k_α^{-1} .

There are also numerical approaches analyzing the edge spin accumulation. Nomura *et al.* (2005) simulated a two-dimensional hole system, using the coupling $H_{\alpha,h}$ [Equation (11)]. They found a spin accumulation that was consistent with the experiments by Wunderlich *et al.* (2005).

4.6 Mesoscopic systems and spin interferometers

So far we have not considered interference effects—e.g., in Sec. 3.4, we used an expansion in lowest order $1/k_F\ell$ which does not include interference between electron propagation paths that follow different trajectories. To include such coherent effects in systems with impurities, one needs to consider the next order in $1/k_F\ell$: the weak localization corrections. Alternatively, one can consider clean systems that are ballistic on length scales of the device. Spin interference effects in mesoscopic

systems open up a new set of technical possibilities, e.g., in rings or ring-like arrays with spin-orbit interaction one can use Berry phase and Aharonov-Casher phase effects to study a variety of phenomena. In the presence of an applied magnetic field, spin-orbit effects can modify the Aharonov-Bohm or Altshuler-Aronov-Spivak oscillations in the electrical conductance. For theoretical discussions, see (Aronov and Lyanda-Geller, 1993; Bulgakov *et al.*, 1999; Engel and Loss, 2000; Frustaglia *et al.*, 2001; Koga *et al.*, 2004; Aeberhard *et al.*, 2005). For experimental results, see (Morpurgo *et al.*, 1998; Yau *et al.*, 2002; Yang *et al.*, 2004; Koga *et al.*, 2006; Koenig *et al.*, 2006; Bagraev *et al.*, 2006).

For practical applications, it is not only important to generate nonequilibrium spin polarization in media with spin orbit coupling, but also inject spin currents produced by such populations into “normal” conductors, i.e., conductors with negligible spin orbit coupling. In normal conductors spin is conserved and spin currents are well defined. Spin injection can be achieved using spin-orbit coupling, even in devices without magnetic fields and without ferromagnetic components. Proposals for such devices, in the mesoscopic regime, have been made by (Kiselev and Kim, 2003; Shekhter *et al.*, 2005; Souma and Nikolić, 2005; Eto *et al.*, 2005; Silvestrov and Mishchenko, 2005).

Generally, spin interference devices make use of the intrinsic and extrinsic spin-orbit couplings presented in Sec. 2 and the spin transport mechanisms discussed in Sec. 3 are important. However, we do not present more concrete descriptions of interference effects or details of microscopic structures; this could be done by solving the Schrödinger equation analytically, by simulating it numerically, or by using weak localization calculations. On the other hand, we can assess the length scales on which spin precession effects are expected: both diffusion equation (Sec. 3.5) and its solution near boundaries (Sec. 4.5) indicate spin precession length $\ell_\alpha = 1/k_\alpha$ as a characteristic length for spin distributions. Furthermore, for clean systems, responses to an inhomogeneous field diverge at the wave vector $q = 2k_\alpha$ of the field (Rashba, 2005). This “breakdown” suggests the length ℓ_α as an optimal size for achieving large spin polarizations. For a more generic Hamiltonian H_{int} , this scale can be estimated as $\ell_{\text{eff}} \sim \hbar^2 k_F / m |\mathbf{b}|$, establishing a “mesoscopic” scale at which one can expect largest static spin responses to electric fields. Because ℓ_{eff} is also of the order of the Dyakonov-Perel spin diffusion length, this estimate seems applicable both to the ballistic and diffusive regimes.

5 Spin Hall effect due to edge states in insulators

In the previous parts of Sec. 4, we discussed spin currents j_y^z driven by electric field E_x , their relevance to spin transport and spin accumulation, and also the techniques for calculating conductivities σ^{SH} [Equation (29)]. Even when these nondiagonal components of the tensor j_j^i were not directly influenced by dissipation, they were calculated for ordinary metallic conductors whose longitudinal electric conductivity σ_{xx} was controlled by electron scattering, hence, electron transport in the bulk was dissipative. More recently, Murakami *et al.* (2004) proposed that some centrosymmetric 3D systems possess properties of “spin insulators.” These are media with

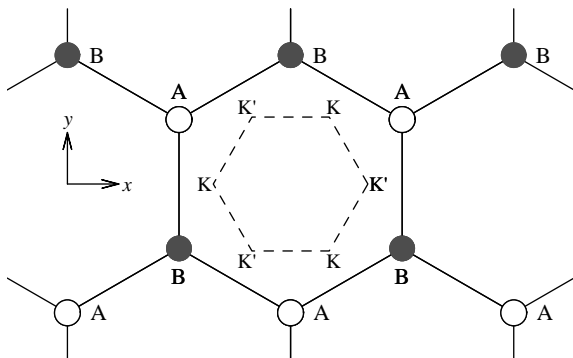


Figure 4: Schematics of honeycomb lattice of graphene. The hexagon in the center is an elementary cell containing two carbon atoms that belong to two sublattices. Atoms of these sublattices are marked as A and B and are shown by empty and filled circles, respectively. Brillouin zone is shown by a dashed line. K and K' indicate nonequivalent corners of the zone where the gap opens.

gapped electron spectra and zero bulk electrical conductivities σ_{xx} but finite and dissipationless spin conductivities σ^{SH} .

The basic idea is as follows. A set of electron bands that in absence of SO coupling belongs to orbital momentum \mathbf{L} , in presence of SO coupling is described by the total angular momentum $\mathbf{J} = \mathbf{L} + \mathbf{S}$. When some of the bands belonging to the \mathbf{J} multiplet are filled, while different bands of the same multiplet are empty and are separated from the filled bands by a gap, all filled bands contribute to spin current. Uniaxially strained zero-gap semiconductors α -Sn and HgTe, and narrow-gap semiconductors of PbTe type were proposed as model systems. Spin conductivity σ^{SH} is large in these materials: it is about $e/\hbar a$ in 3D, a being the lattice constant. In 2D, σ^{SH} is quantized when the Fermi level is inside the gap (Qi *et al.*, 2006; Onoda and Nagaosa, 2005). However, for reasons similar to those discussed in Sec. 4.1, the relation of this σ^{SH} to spin transport is not obvious and was already questioned (Kane and Mele, 2005a; Kane and Mele, 2005b).

A different concept of spin transport in an insulating phase has been developed by Kane and Mele as applied to graphene (Kane and Mele, 2005a; Kane and Mele, 2005b). It is based on the Haldane model of quantum Hall effect (QHE) with spinless fermions under the conditions of zero total magnetic flux across the unit cell (Haldane, 1988). It has been emphasized (Onoda and Nagaosa, 2005; Kane and Mele, 2005a) that this model differs fundamentally from the model by Murakami *et al.* (2004), in particular in the properties of edge channels. Their crucial role for the QHE has been clarified by Halperin (1982), and they play a similar role in the physics of spin Hall effect in graphene. In what follows, we consider properties of graphene in more detail. The graphene model is not only of conceptual interest but is also attractive because of the very recent experimental achievements in measuring electron transport in graphene (Novoselov *et al.*, 2004; Zhang *et al.*, 2005).

Graphene is a monoatomic layer of graphite. Its honeycomb 2D lattice is shown in Fig. 4. The elementary cell includes two atoms shown as A and B. The phase diagram of graphene can be understood from the tight-binding Hamiltonian (Kane and Mele, 2005b)

$$H = t \sum_{\langle ij \rangle} c_i^\dagger c_j + \frac{2i}{\sqrt{3}} \lambda_{SO} \sum_{\langle\langle ij \rangle\rangle} \nu_{ij} c_i^\dagger \sigma_z c_j + i \lambda_R \sum_{\langle ij \rangle} c_i^\dagger (\boldsymbol{\sigma} \times \hat{\mathbf{d}}_{ij})_z c_j + \lambda_v \sum_i \xi_i c_i^\dagger c_i, \quad (36)$$

where c_i are annihilation operators at lattice sites i , spin indices in them being suppressed. The first term is the nearest neighbor hopping term between two sublattices. For the following, of the critical importance is the second term with $\nu_{ij} = (2/\sqrt{3})(\hat{\mathbf{d}}_1 \times \hat{\mathbf{d}}_2)_z = \pm 1$ that describes second neighbor hopping. Here $\hat{\mathbf{d}}_1$ and $\hat{\mathbf{d}}_2$ are unit vectors along two bonds that an electron traverses when going from the site j to the site i . The cross product of $\hat{\mathbf{d}}_1$ and $\hat{\mathbf{d}}_2$ produces a screw that in the Haldane model of spinless fermions couples them to inhomogeneous magnetic flux, while in the present model it couples the orbital motion of an electron to Pauli matrix σ_z . Hence, λ_{SO} is a coupling constant of a mirror symmetric, $z \rightarrow -z$, spin-orbit interaction. The third term is a nearest neighbor Rashba term, $\hat{\mathbf{d}}_{ij}$ being a unit vector in the direction connecting i and j nodes. It explicitly violates $z \rightarrow -z$ symmetry and originates from the coupling to the substrate or from an external electric field. The fourth term is a staggered sublattice potential with ξ_i taking values $\xi_i = \pm 1$ for A and B lattice sites. It vanishes for graphene but would be present for a similar BN film. Including this term is a clue for explaining the difference between the “quantum spin Hall” (QSH) phase and a usual insulator (Kane and Mele, 2005a; Kane and Mele, 2005b).

The remarkable spin properties of graphene are seen from the one-dimensional projection of its energy spectrum, Fig. 5, found by solving the Hamiltonian of Eq. (36) in the geometry of a strip with finite extent in the y -direction (defined in Fig. 4), i.e., having “zig-zag” edges aligned along the x -direction. The spectrum comprises four energy bands, of which the two lower bands are occupied; each bulk band is two-fold spin degenerate. Narrow gaps at K and K' open because of $\lambda_{SO}, \lambda_v \neq 0$ —for $\lambda_{SO}, \lambda_v = 0$, electrons possess a k -linear spectrum of Dirac fermions, $\varepsilon(k) = \hbar c^* k$. In addition to bulk states, there are edge states connecting K and K' bulk continua. Their topology in the panels (a) and (b) is rather different.

In the panel (a) drawn for a small λ_v , edge states traverse the gap. For each edge of the strip, there are two such states. They are Kramers conjugate and propagate in opposite directions. This behavior reflects unusual cross-symmetry of bulk states that manifests itself in the opposite signs of the gap function at K and K' points. The small- λ_v phase has been dubbed as QSH-phase by Kane and Mele (2005a). It is the distinctive property of this phase that at any energy inside the gap there is one pair of edge modes (more generally, an odd number of such pairs).

When $\lambda_R = 0$, σ_z is conserved, and the pattern of dissipationless spin transport become especially simple. Each of independent subsystems of $\sigma_z = \uparrow$ and $\sigma_z = \downarrow$ electrons is equivalent to Haldane spinless fermions (Haldane, 1988). One pair of such “spin filtered” states propagates along each edge. The states with opposite σ_z po-

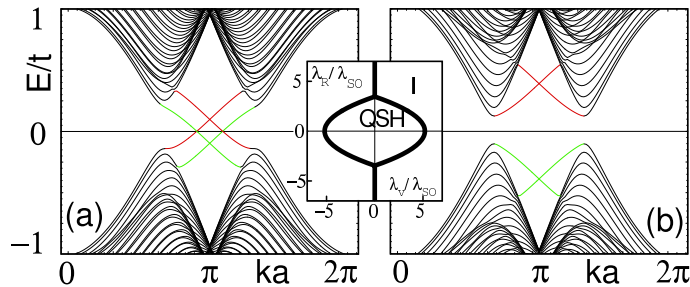


Figure 5: Energy bands of a one-dimensional strip of graphene with “zig-zag” edges, i.e., the strip has finite extent along the y -direction shown in Fig. 4. Narrow gaps in the bulk spectrum are achieved at the K- and K'-vertices of the Brillouin zone. Branches of the spectrum originating from the edges of bulk continua show energies of edge states. Edge states at a given edge of the strip cross at $ka = \pi$, a being the lattice spacing. (a) QSH phase for $\lambda_v = 0.1t$; edge states at a given edge of the strip cross at $ka = \pi$, a being the lattice spacing. (b) A normal insulating phase for $\lambda_v = 0.4t$. In both cases $\lambda_{SO} = 0.06t$ and $\lambda_R = 0.05t$. The inset shows the phase diagram in the λ_v - λ_{SO} -plane for $0 < \lambda_{SO} \ll t$. Reprinted figure with permission from [C.L. Kane and E.J. Mele, Phys. Rev. Lett. **95**, 146802 (2005)]. Copyright (2005) by the American Physical Society.

larizations propagate in opposite directions. Because they form a Kramers doublet, potential backscattering is forbidden and transport is dissipationless. This model predicts two-terminal electric conductivity $G = 2e^2/h$. Propagation of charge current through edge states results in antisymmetric spin accumulation at these edges. In four-terminal geometry, spin currents flow between adjacent contacts, and related spin conductances are quantized; when normalized on a number of transported spins, $G^s = \pm e/2\pi\hbar$. For $\lambda_R \neq 0$, however, σ_z is not conserved. Nevertheless, spin currents persist (if λ_R is small, see below) but they are no longer exactly quantized. An early argument that the spin Hall conductance can be quantized was given by Froehlich *et al.* (1995) when considering incompressible 2D systems.

Panel (b) of Fig. 5, drawn for a larger staggered potential λ_v , shows properties of a normal narrow gap insulator. The gap function has the same sign at K and K', as a result, one pair of edge states runs between two conduction band valleys and the second pair between two valence band valleys. For some boundary conditions at the strip edges, edge states can penetrate the gap. However, there is always an even number of Kramers conjugate pairs of edge states at any given energy inside the gap, hence, backscattering is no longer forbidden. Therefore, it is the topology of edge states that defines the difference between the QSH and insulating phases in a simple and concise form.

The QSH phase is formed due to the bulk spin-orbit coupling λ_{SO} . Increasing asymmetric λ_R or staggered λ_v potentials destroy it when they become large enough. A phase diagram of the competing phases, QSH phase and a normal insulator,

is shown in the inset to Fig. 5. The QSH phase exists inside an ovaloid in the $\lambda_v/\lambda_{SO}-\lambda_R/\lambda_{SO}$ plane. Outside it, graphene shows properties of a normal narrow gap insulator.

Another factor suppressing the gap and spin conductivity is electron scattering in the bulk. Its effect has been investigated numerically by Sheng *et al.* (Sheng, Sheng, Ting and Haldane, 2005) for a four-probe spin Hall setup by using the Landauer-Büttiker formula (Landauer, 1988; Büttiker, 1988); their spin conductivity σ^{SH} describes real spin transport. Disorder was modeled as $\sum_i \epsilon_i c_i^+ c_i$ with ϵ_i randomly distributed in the interval $[-W/2, W/2]$. They found that σ^{SH} remains within a few percent of its quantized value when $W < t$ and the Fermi level stays inside the gap; and σ^{SH} drops fast with increasing W for $W \gtrsim 1.5$. Under the same conditions, σ^{SH} remains stable for $\lambda_R \lesssim 0.2t$. These results allow to establish the parameter range inside which edge spin channels remain robust and carry dissipationless and nearly quantized spin currents. Inside this range, there exist close analogy between QSH and QHE systems.

Currently, there is no direct experimental indications of the spin gap in graphene. A crude theoretical estimate of it by Kane and Mele (2005a) results in the gap $2\Delta_{SO} \sim 2.4$ K what is in a reasonable agreement with different data (Brandt *et al.*, 1988). Meantime, estimates of \hbar/τ based on transport data result in $\hbar/\tau \gtrsim 25$ K for typical mobilities of $\mu \approx 10,000$ cm² V⁻¹ s⁻¹, τ being the momentum relaxation time. Comparison of these data can easily explain suppression of spin-polarized transport through edge channels by disorder in the samples that are currently available. An independent mechanism of suppression is the λ_R constant that develops when electron concentration is controlled by a gate, and the ratio λ_R/λ_{SO} is unknown. Unfortunately, all estimates are crude because electron transport in graphene is still not understood. Novoselov *et al.* (2005) recently reported the minimum metallic conductivity $4e^2/h$ when the Fermi level passes through the conic point of the spectrum; it is nearly independent of the mobility μ . A nonuniversal and even larger conductivity of about $6e^2/h$ was reported by (Zhang *et al.*, 2005). The closest theoretical value $2e^2/h$ comes from the spin channel model (Kane and Mele, 2005a), followed by $4e^2/\pi h$ and $2e^2/\pi h$ found from different models of the bulk transport of Dirac fermions (Ziegler, 1998; Shon and Ando, 1998). Because there exists a region of parameter values where spin transport through edge channels is robust, honeycomb lattices lithographically produced from semiconductors with strong spin-orbit coupling may also be of interest (Zheng and Ando, 2002).

Abanin *et al.* (2006) argued that in the QHE regime, the exchange-enhanced gap for chiral edge modes, originating from Zeeman splitting, may be as large as 100 K. One more system where edge spin channels may play role was proposed by Bernevig and Zhang (2006); it includes parabolic confinement in conjunction with inhomogeneous shear deformation.

6 Acknowledgments

We acknowledge discussions with A.A. Burkov, D. Loss, A.H. MacDonald, C.M. Marcus, E.G. Mishchenko, A.V. Shytov, and R. Winkler. This work was supported

by NSF Grants No. DMR-05-41988 and No. PHY-01-17795, and the Harvard Center for Nanoscale Systems.

References

- Abanin, D. A., Lee, P. A. and Levitov, L. S. (2006). Spin Filtered Edge States and Quantum Hall Effect in Graphene. *Phys. Rev. Lett.*, **96**, 176803.
- Adagideli, I. and Bauer, G. E. W. (2005). Intrinsic Spin Hall Edges. *Phys. Rev. Lett.*, **95**, 256602.
- Aeberhard, U., Wakabayashi, K. and Sigrist, M. (2005). Effect of spin-orbit coupling on zero-conductance resonances in asymmetrically coupled one-dimensional rings. *Phys. Rev. B*, **72**, 075328.
- Ando, T. and Tamura, H. (1992). Conductance fluctuations in quantum wires with spin-orbit and boundary-roughness scattering. *Phys. Rev. B*, **46**, 2332.
- Aronov, A. G. and Lyanda-Geller, Y. B. (1993). Spin-orbit Berry phase in conducting rings. *Phys. Rev. Lett.*, **70**, 343.
- Aronov, A. G., Lyanda-Geller, Y. B. and Pikus, G. E. (1991). Spin polarization of electrons by an electric current. *Sov. Phys. JETP*, **73**, 537.
- Ast, C. R., Pacilé, D., Falub, M., Moreschini, L., Papagno, M., Wittich, G., Wahl, P., Vogelgesang, R., Grioni, M. and Kern, K. (2005). Giant Spin-splitting in the Bi/Ag(111) Surface Alloy. <http://arxiv.org/cond-mat/0509509>.
- Bagraev, N. T., Galkin, N. G., Gehlhoff, W., Klyachkin, L. E., Malyarenko, A. M. and Shelykh, I. A. (2006). Spin interference in silicon one-dimensional rings. *Physica B*, **378**, 894.
- Berger, L. (1970). Side-Jump Mechanism for the Hall Effect of Ferromagnets. *Phys. Rev. B*, **2**, 4559.
- Bernevig, B. A. and Zhang, S.-C. (2004). Intrinsic Spin-Hall Effect in *n*-Doped Bulk GaAs. <http://arxiv.org/cond-mat/0412550>.
- Bernevig, B. A. and Zhang, S.-C. (2006). Quantum Spin Hall Effect. *Phys. Rev. Lett.*, **96**, 106802.
- Bir, G. L. and Pikus, G. E. (1974). *Symmetry and Strain-Induced Effects in Semiconductors*. Wiley, NY.
- Bleibaum, O. (2006). On boundary conditions for spin diffusion equations with Rashba spin-orbit interaction. <http://arxiv.org/cond-mat/0606351>.
- Blount, E. (1962). Formalisms of Band Theory. In *Solid State Physics*, Seitz, F. and Turnbull, D. (Eds). Vol. 13. Academic, NY. p. 305.
- Brandt, N. B., Chudinov, S. M. and Ponomarev, Y. G. (1988). *Semimetals 1. Graphite and its Compounds*. North Holland, Amsterdam.

- Bryksin, V. V. and Kleinert, P. (2006). Theory of electric-field-induced spin accumulation and spin current in the two-dimensional Rashba model. *Phys. Rev. B*, **73**, 165313.
- Bulgakov, E. N., Pichugin, K. N., Sadreev, A. F., Středa, P. and Šeba, P. (1999). Hall-Like Effect Induced by Spin-Orbit Interaction. *Phys. Rev. Lett.*, **83**, 376.
- Burkov, A. A., Núñez, A. S. and MacDonald, A. H. (2004). Theory of spin-charge-coupled transport in a two-dimensional electron gas with Rashba spin-orbit interactions. *Phys. Rev. B*, **70**, 155308.
- Büttiker, M. (1988). Symmetry of electrical conduction. *IBM J. Res. Dev.*, **32**, 317.
- Chalaev, O. and Loss, D. (2005). Spin-Hall conductivity due to Rashba spin-orbit interaction in disordered systems. *Phys. Rev. B*, **71**, 245318.
- Crépieux, A. and Bruno, P. (2001). Theory of the anomalous Hall effect from the Kubo formula and the Dirac equation. *Phys. Rev. B*, **64**, 014416.
- Culcer, D., Sinova, J., Sinitsyn, N. A., Jungwirth, T., MacDonald, A. H. and Niu, Q. (2004). Semiclassical Spin Transport in Spin-Orbit-Coupled Bands. *Phys. Rev. Lett.*, **93**, 046602.
- Dimitrova, O. V. (2005). Spin-Hall conductivity in a two-dimensional Rashba electron gas. *Phys. Rev. B*, **71**, 245327.
- D'yakonov, M. I. and Perel', V. I. (1971). Possibility of orienting electron spins with current. *JETP Lett.*, **13**, 467.
- D'yakonov, M. I. and Perel', V. I. (1972). Spin relaxation of conduction electrons in noncentrosymmetric semiconductors. *Sov. Phys. Solid State*, **13**, 3023.
- Edelstein, V. M. (1990). Spin polarization of conduction electrons induced by electric current in two-dimensional asymmetric electron systems. *Solid State Commun.*, **73**, 233.
- Elliott, R. J. (1954). Theory of the Effect of Spin-Orbit Coupling on Magnetic Resonance in Some Semiconductors. *Phys. Rev.*, **96**, 266.
- Engel, H.-A., Halperin, B. I. and Rashba, E. I. (2005). Theory of Spin Hall conductivity in n-doped GaAs. *Phys. Rev. Lett.*, **95**, 166605.
- Engel, H.-A. and Loss, D. (2000). Conductance fluctuations in diffusive rings: Berry phase effects and criteria for adiabaticity. *Phys. Rev. B*, **62**, 10238.
- Engel, H.-A., Rashba, E. I. and Halperin, B. I. (2006). Out-of-plane spin polarization from in-plane electric and magnetic fields. <http://arxiv.org/cond-mat/0609078>.
- Entin-Wohlman, O., Aharony, A., Galperin, Y. M., Kozub, V. I. and Vinokur, V. (2005). Orbital ac Spin-Hall Effect in the Hopping Regime. *Phys. Rev. Lett.*, **95**, 086603. And references therein.

- Erlingsson, S. I., Schliemann, J. and Loss, D. (2005). Spin susceptibilities, spin densities, and their connection to spin currents. *Phys. Rev. B*, **71**, 035319.
- Eto, M., Hayashi, T. and Kurotani, Y. (2005). Spin Polarization at Semiconductor Point Contacts in Absence of Magnetic Field. *J. Phys. Soc. Jpn.*, **74**, 1934.
- Froehlich, J., Studer, U. and Thiran, E. (1995). Quantum Theory of Large Systems of Non-Relativistic Matter. <http://arxiv.org/cond-mat/9508062>.
- Frustaglia, D., Hentschel, M. and Richter, K. (2001). Quantum Transport in Nonuniform Magnetic Fields: Aharonov-Bohm Ring as a Spin Switch. *Phys. Rev. Lett.*, **87**, 256602.
- Galitski, V. M., Burkov, A. A. and Das Sarma, S. (2006). Boundary conditions for spin diffusion. <http://arxiv.org/cond-mat/0601677>.
- Ganichev, S. D. and Prettl, W. (2003). Spin photocurrents in quantum wells. *J. Phys.: Condens. Matter*, **15**, R935.
- Ganichev, S., Danilov, S., Schneider, P., Bel'kov, V., Golub, L., Wegscheider, W., Weiss, D. and Prettl, W. (2006). Electric current-induced spin orientation in quantum well structures. *J. Magn. Magn. Mater.*, **300**, 127.
- Glazov, M. M. and Ivchenko, E. L. (2002). Precession spin relaxation mechanism caused by frequent electron-electron collisions. *JETP Lett.*, **75**, 403.
- Govorov, A. O., Kalameitsev, A. V. and Dulka, J. P. (2004). Spin-dependent transport of electrons in the presence of a smooth lateral potential and spin-orbit interaction. *Phys. Rev. B*, **70**, 245310.
- Grimaldi, C., Cappelluti, E. and Marsiglio, F. (2006). Off-Fermi surface cancellation effects in spin-Hall conductivity of a two-dimensional Rashba electron gas. *Phys. Rev. B*, **73**, 081303.
- Haldane, F. D. M. (1988). Model for a Quantum Hall Effect without Landau Levels: Condensed-Matter Realization of the "Parity Anomaly". *Phys. Rev. Lett.*, **61**, 2015.
- Halperin, B. I. (1982). Quantized Hall conductance, current-carrying edge states, and the existence of extended states in a two-dimensional disordered potential. *Phys. Rev. B*, **25**, 2185.
- Hankiewicz, E. M. and Vignale, G. (2006). Spin Coulomb drag corrections to the extrinsic spin-Hall effect of a two-dimensional electron gas. *Phys. Rev. B*, **73**, 115339.
- Hirsch, J. E. (1999). Spin Hall Effect. *Phys. Rev. Lett.*, **83**, 1834.
- Huang, H. C., Voskoboynikov, O. and Lee, C. P. (2003). Spin-orbit interaction and electron elastic scattering from impurities in quantum wells. *Phys. Rev. B*, **67**, 195337.

- Inoue, J. I., Bauer, G. E. W. and Molenkamp, L. W. (2004). Suppression of the persistent spin Hall current by defect scattering. *Phys. Rev. B*, **70**, 041303.
- Ivchenko, E. L. and Pikus, G. (1978). New photogalvanic effect in gyrotropic crystals. *JETP Lett.*, **27**, 604.
- Ivchenko, E. and Pikus, G. (1997). *Superlattices and Other Heterostructures*. Springer, Berlin.
- Kane, C. L. and Mele, E. J. (2005a). Quantum Spin Hall Effect in Graphene. *Phys. Rev. Lett.*, **95**, 226801.
- Kane, C. L. and Mele, E. J. (2005b). Z_2 Topological Order and the Quantum Spin Hall Effect. *Phys. Rev. Lett.*, **95**, 146802.
- Kato, Y. K., Myers, R. C., Gossard, A. C. and Awschalom, D. D. (2004a). Current-Induced Spin Polarization in Strained Semiconductors. *Phys. Rev. Lett.*, **93**, 176601.
- Kato, Y. K., Myers, R. C., Gossard, A. C. and Awschalom, D. D. (2004b). Observation of the Spin Hall Effect in Semiconductors. *Science*, **306**, 1910.
- Khaetskii, A. (2006). Intrinsic spin current for an arbitrary Hamiltonian and scattering potential. *Phys. Rev. B*, **73**, 115323.
- Kiselev, A. A. and Kim, K. W. (2003). T-shaped spin filter with a ring resonator. *J. Appl. Phys.*, **94**, 4001.
- Koenig, M., Tschetschetkin, A., Hankiewicz, E., Sinova, J., Hock, V., Daumer, V., Schaefer, M., Becker, C., Buhmann, H. and Molenkamp, L. (2006). Direct observation of the Aharonov-Casher phase. *Phys. Rev. Lett.*, **96**, 076804.
- Koga, T., Nitta, J. and van Veenhuizen, M. (2004). Ballistic spin interferometer using the Rashba effect. *Phys. Rev. B*, **70**, 161302.
- Koga, T., Sekine, Y. and Nitta, J. (2006). Experimental realization of a ballistic spin interferometer based on the Rashba effect using a nanolithographically defined square loop array. *Phys. Rev. B*, **74**, 041302.
- Krotkov, P. and Das Sarma, S. (2006). Intrinsic spin Hall conductivity in a generalized Rashba model. *Phys. Rev. B*, **73**, 195307.
- Landauer, R. (1988). Spatial variation of currents and fields due to localized scatterers in metallic conduction. *IBM J. Res. Dev.*, **32**, 306.
- Levitov, L. S., Nazarov, Y. N. and Eliashberg, G. M. (1985). Magnetoelectric effects in conductors with mirror isomer symmetry. *Sov. Phys. JETP*, **61**, 133.
- Lewiner, C., Betbeder, O. and Nozières, P. (1973). Field theoretical approach to anomalous Hall-effect in semiconductors. *J. Phys. Chem. Solids*, **34**, 765.

- Li, J., Hu, L. and Shen, S.-Q. (2005). Spin-resolved Hall effect driven by spin-orbit coupling. *Phys. Rev. B*, **71**, 241305.
- Liu, S. Y. and Lei, X. L. (2005). Disorder effects on the spin-Hall current in a diffusive Rashba two-dimensional heavy-hole system. *Phys. Rev. B*, **72**, 155314; **72**, 249901(E).
- Mal'shukov, A. G. and Chao, K. A. (2005). Spin Hall conductivity of a disordered two-dimensional electron gas with Dresselhaus spin-orbit interaction. *Phys. Rev. B*, **71**, 121308.
- Mal'shukov, A. G., Wang, L. Y., Chu, C. S. and Chao, K. A. (2005). Spin Hall Effect on Edge Magnetization and Electric Conductance of a 2D Semiconductor Strip. *Phys. Rev. Lett.*, **95**, 146601.
- Meier, F. and Zakharchenya, B. P. (Eds) (1984). *Optical Orientation*. North Holland.
- Mishchenko, E. G., Shytov, A. V. and Halperin, B. I. (2004). Spin Current and Polarization in Impure Two-Dimensional Electron Systems with Spin-Orbit Coupling. *Phys. Rev. Lett.*, **93**, 226602.
- Morpurgo, A. F., Heida, J. P., Klapwijk, T. M., van Wees, B. J. and Borghs, G. (1998). Ensemble-Average Spectrum of Aharonov-Bohm Conductance Oscillations: Evidence for Spin-Orbit-Induced Berry's Phase. *Phys. Rev. Lett.*, **80**, 1050.
- Mott, N. F. (1936). The electrical conductivity of transition metals. *Proc. Roy. Soc. (London) A*, **153**, 699.
- Mott, N. F. and Massey, H. S. W. (1965). *The Theory of Atomic Collisions*. Oxford University Press, London.
- Motz, J. W., Olsen, H. and Koch, H. W. (1964). Electron Scattering without Atomic or Nuclear Excitation. *Rev. Mod. Phys.*, **36**, 881. Sec. VI and Eqs. (1A-107) and (1A-403).
- Murakami, S. (2004). Absence of vertex correction for the spin Hall effect in *p*-type semiconductors. *Phys. Rev. B*, **69**, 241202.
- Murakami, S., Nagaosa, N. and Zhang, S.-C. (2003). Dissipationless Quantum Spin Current at Room Temperature. *Science*, **301**, 1348.
- Murakami, S., Nagaosa, N. and Zhang, S.-C. (2004). Spin-Hall Insulator. *Phys. Rev. Lett.*, **93**, 156804.
- Nagaosa, N. (2006). Anomalous Hall Effect – A New Perspective. *J. Phys. Soc. Jpn*, **75**, 042001.
- Nikolić, B. K., Zârbo, L. P. and Souma, S. (2005). Mesoscopic spin Hall effect in multiprobe ballistic spin-orbit-coupled semiconductor bridges. *Phys. Rev. B*, **72**, 075361.

- Nomura, K., Wunderlich, J., Sinova, J., Kaestner, B., MacDonald, A. and Jungwirth, T. (2005). Edge spin accumulation in semiconductor two-dimensional hole gases. *Phys. Rev. B*, **72**, 245330.
- Novoselov, K. S., Geim, A. K., Morozov, S. V., Jiang, D., Katsnelson, M. I., Grigorieva, I. V., Dubonos, S. V. and Firsov, A. A. (2005). Two-dimensional gas of massless Dirac fermions in graphene. *Nature*, **438**, 197.
- Novoselov, K. S., Geim, A. K., Morozov, S. V., Jiang, D., Zhang, Y., Dubonos, S. V., Grigorieva, I. V. and Firsov, A. A. (2004). Electric Field Effect in Atomically Thin Carbon Films. *Science*, **306**, 666.
- Nozières, P. and Lewiner, C. (1973). A simple theory of the anomalous Hall effect in Semiconductors. *J. Phys. (Paris)*, **34**(10), 901.
- Onoda, M. and Nagaosa, N. (2005). Spin Current and Accumulation Generated by the Spin Hall Insulator. *Phys. Rev. Lett.*, **95**, 106601.
- Pikus, G. E. and Titkov, A. N. (1984). Spin Relaxation under Optical Orientation in Semiconductors. In *Optical Orientation*, Meier, F. and Zakharchenya, B. P. (Eds). North Holland. Chapter 3, p. 73.
- Qi, X.-L., Wu, Y.-S. and Zhang, S.-C. (2006). Topological Quantization of the Spin Hall Effect. *Phys. Rev. B*, **74**, 085308.
- Raimondi, R. and Schwab, P. (2005). Spin-Hall effect in a disordered two-dimensional electron system. *Phys. Rev. B*, **71**, 033311.
- Rashba, E. I. (2003). Spin currents in thermodynamic equilibrium: The challenge of discerning transport currents. *Phys. Rev. B*, **68**, 241315.
- Rashba, E. I. (2004). Sum rules for spin Hall conductivity cancellation. *Phys. Rev. B*, **70**, 201309.
- Rashba, E. I. (2005). Spin Dynamics and Spin Transport. *J. Supercond.*, **18**, 137.
- Rashba, E. I. (2006). Spin-orbit coupling and spin transport. *Physica E*, **34**, 31.
- Schliemann, J. and Loss, D. (2005). Spin-Hall transport of heavy holes in III-V semiconductor quantum wells. *Phys. Rev. B*, **71**, 085308.
- Shchelushkin, R. V. and Brataas, A. (2005). Spin Hall effects in diffusive normal metals. *Phys. Rev. B*, **71**, 045123.
- Shekhter, A., Khodas, M. and Finkel'stein, A. M. (2005). Diffuse emission in the presence of an inhomogeneous spin-orbit interaction for the purpose of spin filtration. *Phys. Rev. B*, **71**, 125114.
- Sheng, D. N., Sheng, L., Weng, Z. Y. and Haldane, F. D. M. (2005). Spin Hall effect and spin transfer in a disordered Rashba model. *Phys. Rev. B*, **72**, 153307.

- Sheng, L., Sheng, D. N. and Ting, C. S. (2005). Spin-Hall Effect in Two-Dimensional Electron Systems with Rashba Spin-Orbit Coupling and Disorder. *Phys. Rev. Lett.*, **94**, 016602.
- Sheng, L., Sheng, D. N., Ting, C. S. and Haldane, F. D. M. (2005). Nondissipative Spin Hall Effect via Quantized Edge Transport. *Phys. Rev. Lett.*, **95**, 136602.
- Shi, J., Zhang, P., Xiao, D. and Niu, Q. (2006). On A Proper Definition of Spin Current. *Phys. Rev. Lett.*, **96**, 076604.
- Shon, N. H. and Ando, T. (1998). Quantum Transport in Two-Dimensional Graphite System. *J. Phys. Soc. Japan*, **67**, 2421.
- Shytov, A. V., Mishchenko, E. G., Engel, H.-A. and Halperin, B. I. (2006). Small-angle impurity scattering and the spin Hall conductivity in two-dimensional semiconductor systems. *Phys. Rev. B*, **73**, 075316.
- Sih, V., Myers, R. C., Kato, Y. K., Lau, W. H., Gossard, A. C. and Awschalom, D. D. (2005). Spatial imaging of the spin Hall effect and current-induced polarization in two-dimensional electron gases. *Nature Phys.*, **1**, 31.
- Silov, A. Y., Blajnov, P. A., Wolter, J. H., Hey, R., Ploog, K. H. and Averkiev, N. S. (2004). Current-induced spin polarization at a single heterojunction. *Appl. Phys. Lett.*, **85**, 5929.
- Silvestrov, P. G. and Mishchenko, E. G. (2005). Polarized Electric Current in Semiclassical Transport with Spin-Orbit Interaction. <http://arxiv.org/cond-mat/0506516>.
- Sinova, J., Culcer, D., Niu, Q., Sinitsyn, N. A., Jungwirth, T. and MacDonald, A. H. (2004). Universal Intrinsic Spin Hall Effect. *Phys. Rev. Lett.*, **92**, 126603.
- Sinova, J., Murakami, S., Shen, S.-Q. and Choi, M.-S. (2006). Spin-Hall effect: Back to the Beginning on a Higher Level. *Solid State Comm.*, **138**, 214.
- Smit, J. (1958). The spontaneous Hall effect in ferromagnetics-II. *Physica*, **24**, 39.
- Souma, S. and Nikolić, B. K. (2005). Spin Hall Current Driven by Quantum Interferences in Mesoscopic Rashba Rings. *Phys. Rev. Lett.*, **94**, 106602.
- Stern, N. P., Ghosh, S., Xiang, G., Zhu, M., Samarth, N. and Awschalom, D. D. (2006). Current-Induced Polarization and the Spin Hall Effect at Room Temperature. <http://arxiv.org/cond-mat/0607288>.
- Trebin, H. R., Rössler, U. and Ranvaud, R. (1979). Quantum resonances in the valence bands of zinc-blende semiconductors. I. Theoretical aspects. *Phys. Rev. B*, **20**, 686.
- Tse, W.-K. and Das Sarma, S. (2006). Spin Hall Effect in Doped Semiconductor Structures. *Phys. Rev. Lett.*, **96**, 056601.

- Usaj, G. and Balseiro, C. A. (2005). Spin accumulation and equilibrium currents at the edge of 2DEGs with spin-orbit coupling. *Europhys. Lett.*, **72**, 631.
- Valenzuela, S. O. and Tinkham, M. (2006). Direct electronic measurement of the spin Hall effect. *Nature*, **442**, 176.
- Vas'ko, F. T. and Prima, N. A. (1979). Spin splitting of spectrum of two-dimensional electrons. *Sov. Phys. Solid State*, **21**, 994.
- Winkler, R. (2000). Rashba spin splitting in two-dimensional electron and hole systems. *Phys. Rev. B*, **62**, 4245.
- Winkler, R. (2003). *Spin-Orbit Coupling Effects in Two-Dimensional Electron and Hole System*. Springer, Berlin.
- Wunderlich, J., Kaestner, B., Sinova, J. and Jungwirth, T. (2005). Experimental Observation of the Spin-Hall Effect in a Two-Dimensional Spin-Orbit Coupled Semiconductor System. *Phys. Rev. Lett.*, **94**, 047204.
- Yafet, Y. (1963). g -factors and spin-lattice relaxation of conduction electrons. In *Solid State Physics*, Seitz, F. and Turnbull, D. (Eds). Vol. 14. Academic, NY. p. 1.
- Yang, M. J., Yang, C. H. and Lyanda-Geller, Y. B. (2004). Quantum beating in ring conductance: Observation of spin chiral states and Berry's phase. *Europhys. Lett.*, **66**, 826.
- Yau, J.-B., Poortere, E. P. D. and Shayegan, M. (2002). Aharonov-Bohm Oscillations with Spin: Evidence for Berry's Phase. *Phys. Rev. Lett.*, **88**, 146801.
- Zhang, S. (2000). Spin Hall Effect in the Presence of Spin Diffusion. *Phys. Rev. Lett.*, **85**, 393.
- Zhang, S. and Yang, Z. (2005). Intrinsic Spin and Orbital Angular Momentum Hall Effect. *Phys. Rev. Lett.*, **94**, 066602.
- Zhang, Y., Tan, Y.-W., Stormer, H. L. and Kim, P. (2005). Experimental observation of the quantum Hall effect and Berry's phase in graphene. *Nature*, **438**, 201.
- Zheng, Y. and Ando, T. (2002). Hall conductivity of a two-dimensional graphite system. *Phys. Rev. B*, **65**, 245420.
- Ziegler, K. (1998). Delocalization of 2D Dirac Fermions: The Role of a Broken Supersymmetry. *Phys. Rev. Lett.*, **80**, 3113.